Technische Universität München
Department of Civil, Geo and Environmental Engineering
Chair of Cartography
Prof. Dr. -Ing. Liqiu Meng

The Effect of Satellite Image Resolution and Minimum Mapping Unit on the Accuracy of Forest Cover Maps

Aleksandra Draksler

Master's Thesis

Study Course:	Cartography M.Sc.
Supervisors:	Dr. Pablo Rosso
	Juliane Cron M.Sc.
	Prof. Dr. -Ing. Liqiu Meng
Cooperation:	Planet
Submitted:	March 28, 2017

DECLARATION OF AUTHORSHIP

I hereby declare that the submitted master thesis entitled **The Effect of Satellite Image Resolution and Minimum Mapping Unit on the Accuracy of Forest Cover Maps** is my own work and that, to the best of my knowledge, it contains no material previously published, or substantially overlapping with material submitted for the award of any other degree at any institution, except where acknowledgement is made in the text.

Berlin, 28th of March 2017 Aleksandra Draksler

ABSTRACT

Reducing emissions from deforestation and forest degradation (REDD+) mechanism requires high-quality forest cover maps to determine changes in forest cover and consequent forest carbon emissions. The accuracy of forest cover maps can be affected by utilised satellite imagery spatial resolution for mapping forest and minimum mapping unit (MMU) at which forest cover is mapped. In this Master's thesis first, the effect of high- and medium-resolution satellite imagery on the accuracy of derived forest cover maps was tested and quantified. Second, various MMU sizes were tested to measure the magnitude of changed accuracy at increasing MMU when mapping forest. Accuracy tests were conducted on two test sites in Ethiopia and Peru. Prior to testing forest cover was mapped based on different forest mapping methodologies for high- and medium-resolution satellite imagery. Accuracy assessment results show that in order to generate highly accurate forest cover maps high-resolution satellite imagery needs to be employed for forest cover mapping. Furthermore, the research confirmed that the quality of forest cover maps decreases by increasing MMU. Therefore, it is recommended for countries participating in REDD+ to consider the effect of satellite image resolution and MMU on the forest cover mapping accuracy when selecting satellite sensor and operational MMU for mapping forest cover.

Keywords: Forest Cover Mapping, Accuracy Assessment, Minimum Mapping Unit

TABLE OF CONTENTS

LIST OF TABLES

LIST OF FIGURES

ABBREVIATIONS

REDD+	Reducing Emissions from Deforestation and Forest Degradation
MMU	Minimum Mapping Unit
UNFCCC	United Nations Framework Convention on Climate Change
MRV	Measurement, Reporting and Veriffcation
ForMoSa	Forest Degradation Monitoring with Satellite Data
FAO	Food and Agriculture Organisation of the United Nations
ESA	European Space Agency
AutoMCU	Automated Monte Carlo Unmixing
SNNPR	Southern Nations, Nationalities and People's region
UTM	Universal Transverse Mercator
OLI	Operational Land Imager
TIRS	Thermal Infrared Sensor
MSI	Multispectral Instrument
ToA	Top-of-atmosphere
CART	Classification and Regression Tree
SMA	Spectral mixing analysis

1 INTRODUCTION

1.1 Introduction and context

Forest carbon emissions constitute approximately 17% of the global carbon footprint [1]. Reducing greenhouse gas emissions associated with forest disturbance and thus enhancing forest carbon storage is the main aim of the United Nations collaborative programme on Reducing emissions from deforestation and forest degradation (UN-REDD). REDD+ is a mechanism developed by United Nations Framework Convention on Climate Change (UNFCCC) and is supported by the UN-REDD programme. Not only REDD+ activities focus on reducing deforestation and degradation, but also include forest enhancement, its sustainable management and conservation. REDD+ as mechanism offers a result-based payment for forest preservation in developing countries that undertake REDD+ activities [1], [2].

The three components, Measurement, Reporting and Verification (MRV) are essential to implement the REDD+ mechanism successfully. Measurement is the step in which basic datasets are collected over time and used to quantify greenhouse gas emissions based on forest area change. Field measurements and observations, detection through remote sensing and interviews are possible data sources. In reporting process measurement, results are presented to the UNFCCC based on established formats and standards. Reported measurements need to be independently verified for sufficient accuracy and reliability by an external reviewer [3].

Satellite remote sensing is a powerful tool for monitoring and mapping forest cover changes to support the REDD+ measurement component. Its continuous monitoring over large areas enables detection and accurate estimation of changes in forest area (i.e. deforestation and forest degradation) and carbon stocks. To detect and measure forest changes the information about the forest cover within the area of interest at the end and

at the beginning of monitoring period is essential [2]. A crucial element of forest cover mapping is the delimiting criteria of what constitutes forest and what not. UNFCCC defines forest as a minimum area of land of 0.5-1.0 hectares with the tree crown cover of more than 10-30% where trees have the potential to reach a minimum height of 2-5 meters at maturity [4]. It is necessary for countries participating in REDD+ to establish clear national forest definition according to above mentioned UNFCCC's guidelines.

Carbon stock changes can be quantified accurately only if forest cover is mapped with high accuracy. Different variables included in forest cover mapping might affect the forest cover map quality. However, there are two main aspects this Master's thesis focuses on. The first is the sensor's spatial and spectral resolutions, which among other issues, determines the proportion of mixed tree/non-tree pixels and consequently, the degree of uncertainty in the classification. The second factor is the unit at which the minimum forest area is computed. This Minimum Mapping Unit (MMU), is operationally defined and it is not necessarily related to the sensor(s) utilized for monitoring.

Forest Degradation Monitoring with Satellite Data (ForMoSa) is an ongoing project carried out in cooperation with Planet company, Wageningen University, Food and Agriculture Organisation of the United Nations (FAO) and European Space Agency (ESA). ForMoSa focuses on delivering products of high precision generated from high spatial resolution satellite data. Also, to ensure high temporal revisit and a longer monitoring period, sensor interoperability combining RapidEye, Sentinel-2 and Landsat 8 imagery is being tested. One of the important intermediate information layers in ForMoSa are forest cover maps, which are the basis for subsequent forest change detection. This Master's thesis research was conducted in the scope of ForMoSa project at Planet company [5].

1.2 Motivation and problem statement

It is not well established yet how the accuracy of forest cover maps varies in relation to the spatial and spectral resolution of satellite data and possible MMU utilized for mapping forest. Firstly, REDD+ requires highly accurate forest cover maps to determine changes in forest cover. The effect of spatial resolution on map accuracy and its consequences on the efficacy of the monitoring plan at high- and medium-resolution satellite imagery still needs to be determined. Secondly, forest definition in REDD+ requires the establishment of a MMU at which the crown cover threshold is applied to determine the presence or absence of forest at a given location. The choice of MMU may have a significant impact on the accuracy of the forest cover map. This Master's thesis addresses the effect of different MMUs, pixel sizes and spectral resolutions on the accuracy of forest cover maps for REDD+ MRV projects. Quantifying the accuracy of forest cover maps can help REDD+ countries decide on the satellite imagery spatial resolution and MMU to be used for monitoring deforestation and forest degradation.

1.3 Research questions and hypotheses

To address the above mentioned two research problems, the following research questions need to be answered:

- How do different high- and medium-resolution satellite sensors affect the accuracy of forest cover mapping? What is the effect of mixed pixels in medium-resolution imagery on the accuracy of forest maps with respect to high-resolution imagery?
- How does the size of MMUs affect the accuracy of forest cover mapping? How much does accuracy vary when increasing the MMU for mapping forest?

From the two research questions the following hypotheses can be formulated:

- The overall accuracy of forest cover maps derived from the error matrix decreases with decreasing resolution of satellite imagery used to map forest. The degree of classification uncertainty caused by a high proportion of mixed pixels in medium-resolution satellite imagery increases with respect to high-resolution imagery.

- The overall accuracy of forest cover maps derived from the error matrix decreases with increasing size of the MMU used for mapping forest. Therefore, noticeable accuracy differences can be observed when comparing forest cover maps generated based on small MMU and the ones derived from big MMU.

1.4 Structure of the thesis

This thesis consists of six chapters. The first chapter introduces the topic, identifies the research and gives an overview of the thesis structure. The next chapter reviews previously published works on forest cover mapping, MMU and accuracy assessment. In the third chapter study areas and data used for the research are described. The fourth chapter focuses on the methodology used to map forest cover and design tests to assess the accuracy of derived forest cover maps. Chapter five presents, evaluates and discusses test results. The last chapter, chapter six concludes the research and describes possible future work.

2 THEORETICAL BACKGROUND

In the first part of this chapter, two distinctive methodologies for mapping forest cover with remote sensing are reviewed. The second part of the review focuses on previous research on the effect of MMU in forest mapping. The last part of the chapter gives a detailed overview of remote sensing accuracy assessment and describes its main components.

2.1 Forest mapping with remote sensing data

Numerous approaches and methodologies are used by researchers to address the forest cover mapping problem with remote sensing data. Forest cover is mapped based on criteria specified by the forest definition and include crown cover threshold, minimum tree height and MMU. To be able to map forest considering forest definition criteria the tree cover needs to be extracted from the original image. Generally, the extraction of tree cover and consequent forest cover mapping methodology differs on the satellite imagery resolution used. Therefore, two different approaches for mapping forest, first from high-resolution, and second from medium-resolution satellite data are reviewed.

The framework presented in [6] by Magdon et. al. uses high-resolution RapidEye satellite imagery to generate forest cover maps. This framework is based on hierarchical classification scheme consisting of three levels. The first level output is a land cover map with 14 classes, the second level outputs FAO based land use map with 5 land use classes and the third level is a forest/non-forest map. The Random Forest classification algorithm is used to classify original RapidEye image and thus derive the level 1 land cover map. The three specific forest definition variables, minimum mapping area, minimum tree height and minimum crown cover threshold are applied to the level 1 map by designed decision tree. Based on this decision tree each image pixel is classified to one of

the FAO defined land use classes. Finally, the level 2 land use classes are aggregated to generate the level 3 forest/non-forest cover map. Additionally, Magdon et. al. supports the development of classification framework by testing it on two diverse tropical regions. Conducted accuracy assessment confirmed suitability of high-resolution RapidEye imagery for forest cover mapping and applicability of classification framework for forest mapping of smaller regions. Moreover, it is possible to implement any minimum mapping area, crown cover threshold, classification algorithm and high-resolution satellite imagery into the designed framework.

In [7] Asner et. al. describes a fully automated system for mapping forest cover, deforestation and forest disturbance applicable for forest monitoring in REDD+. CLASlite software was designed to be used especially by non-experts and it integrates various algorithms to map forest cover and its changes. CLASlite sub-pixel decomposition method based on Automated Monte Carlo Unmixing (AutoMCU) process uses spectral signatures of different medium- and low-resolution satellite sensors to calculate fractions of surface covers. CLASlite output fraction image defines the percentage of three so-called endmembers, live vegetation, dead vegetation and bare substrate in each image pixel. The composition of each image pixel is defined by solving a linear equation for each satellite image band based on known endmembers spectra. Field measurements and hyperspectral satellite imagery were the sources for deriving the three endmembers spectra used in AutoMCU analysis. Besides the cover fraction, pixel decomposition method outputs standard deviation images for each endmember fraction estimate and a pixel based root mean squared error image. Land cover fractions are then used to automatically map forest cover using single image analysis or to map deforestation and forest disturbances by analysing multiple images. Endmembers fractions of a single image are finally thresholded based on developed decision tree to map forest and non-forest cover.

For this Master's thesis study forest cover mapping approaches similar to Magdon's and

Asner's were adapted to map forest from high- and medium-resolution satellite imagery, respectively. The main reason to select these two specific methodologies was that they are applicable for mapping forest based on high- and medium-resolution satellite data used for this research. Adapted forest cover mapping approaches are in detail explained in chapter 4.2.

2.2 Minimum mapping unit in forest cover mapping

Forest area on forest cover maps must be defined based on a clear forest definition that establishes the threshold between forest and non-forest. National forest definitions need to define the minimum tree crown cover and the reference area on which the crown cover threshold is applied. However, the reference area chosen might significantly affect the accuracy of generated forest cover maps. The reference area represents the minimum unit at which forest cover is mapped and is in this Master's thesis referred to as MMU.

Kleinn [8] analysed the relationship between crown cover threshold and MMU with respect to the forest cover area estimates. Analysis of a simulation and an air photo showed that different MMUs and percent crown cover affect total forest cover area estimates. The results supported by air photo based analysis confirmed that small crown cover threshold values and increasing MMU increase the forest cover area estimates. Conversely, high crown cover threshold values and increasing MMUs decrease the forest cover estimates. For fixed MMU and increasing crown cover threshold, decreasing forest cover area estimates were observed. Based on the air photo analysis, up to 10% differences of forest cover area estimates were detected when MMU was doubled and the crown cover thresholds were low. However, forest cover area estimates for 50% crown cover threshold and increasing MMU were stable.

The research of Magdon and Kleinn [9] investigated the MMU and crown cover threshold relationship on forest edge models. The research based on artificially generated tree cover

maps showed that land cover estimates are not only affected by MMU and minimum crown cover but also forest fragmentation, crown cover proportion and spatial resolution. As can be seen in Figure 1 different MMU sizes and fixed crown cover threshold affect the proportion of forest mapped and its pattern. Additional results showed that both crown cover threshold and MMU have a greater impact on the forest cover estimates in areas with high level of forest fragmentation than in compact ones. Moreover, Magdon and Kleinn [9] show that the effect of spatial resolution is a function of the crown cover threshold and the level of forest fragmentation. Nevertheless, the effect of spatial resolution on the forest cover estimates is only minor compared to other investigated variables like MMU, crown cover threshold, landscape composition and fragmentation.

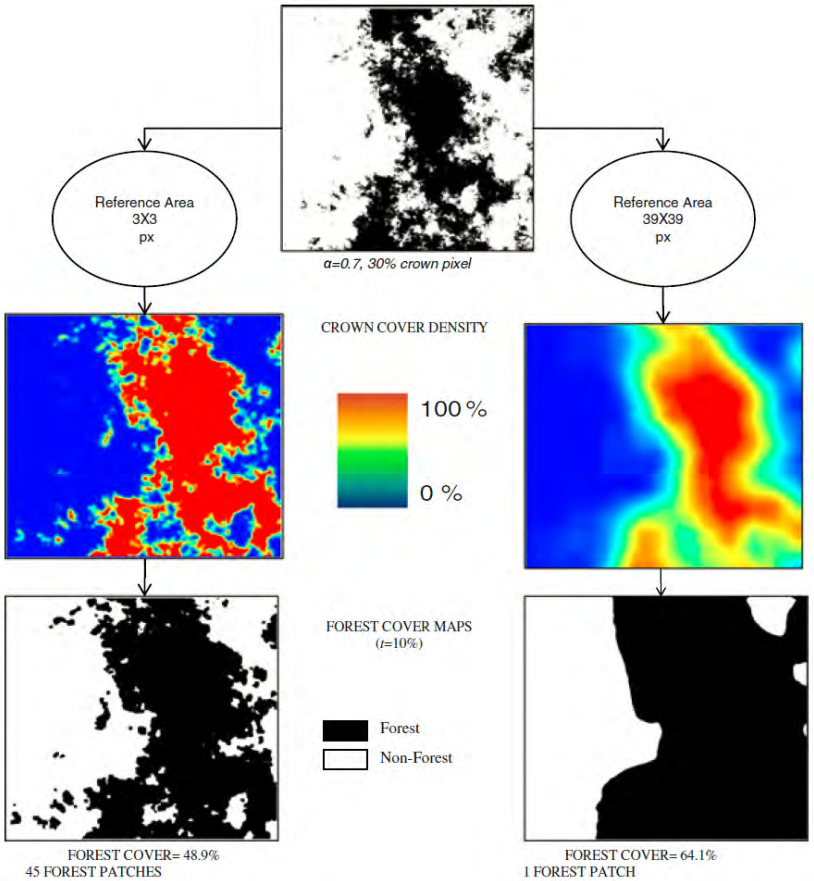

Figure 1: Results of forest cover mapping for a highly fragmented landscape $\alpha = 0.7$ with 30% crown pixels and a crown cover threshold of $t = 0.1$. Source: [9]

.

Research done by Magdon and Kleinn shows that variables such as MMU, crown cover percent, forest fragmentation, crown cover proportion and spatial resolution affect forest cover area estimates. However, the impact of MMU on the accuracy of forest cover maps specifically was not in focus of above mentioned studies and is, therefore, the research topic of this Master's thesis and is described in more detail in chapter 4.3.3.

2.3 Accuracy assessment of remotely sensed data

Scientific research, policy and decision making are often based on thematic maps derived from remotely sensed data. Therefore, these maps should undergo statistically rigorous accuracy assessment [10]. According to some definitions, accuracy measures the bias of an estimator or calculated value which tells us how much the estimated value differs from the true value. Map accuracy is a variable of both, positional and thematic accuracy. Thematic accuracy considers the map feature labels and measures the agreement between the feature labels on the map and the feature labels from the reference data. When assessing the thematic accuracy derived map data and reference data are compared in the error matrix also known as confusion matrix [11].

According to [10], three main components of rigorous accuracy assessment should be considered:

- The sampling design
- The response design
- The analysis

Accuracy assessment of remotely sensed data should include above listed components explained in more detail in sections 2.3.1 to 2.3.3. However, up to now, no standardized

accuracy assessment protocols are available in the literature. Instead, the good practice recommends analysts to adapt accuracy assessment design and analysis considering accuracy assessment objectives and purpose. The main considerations are cost-effectiveness, simplicity and statistical rigour. Prior to accuracy assessment, processed thematic maps need to be visually inspected for obvious errors. Visually detected errors should be removed before conducting accuracy assessment [12], [10].

2.3.1 Sampling design

In [12] sampling design is described as a protocol that selects a sample of spatial units from the map. Based on selected number of samples accuracy assessment is performed. Sampling design requires selection of probability sampling design, the sampling unit and the sample size [10], [11], [13].

It is necessary to choose probability sampling design that selects random samples from the population with inclusion probabilities greater than zero. If inclusion probability is above zero, the selected samples represent an entire region of the map and accuracy assessment is valid [10], [13]. There are simple random, stratified random, systematic and cluster sampling used in accuracy assessment [10].

Simple random sampling randomly selects sample units from the classified map. Each sample unit is chosen without bias, which is a very good statistical property of simple random sampling approach. The disadvantage of this sampling scheme is that it tends to undersample rare map categories [11].

Stratified random sampling method divides map area into strata according to mapped classes. Since samples are obtained from strata all map classes, including rare ones are represented in the accuracy assessment [11].

Systematic sampling protocol collects samples at a regular interval after the first

sample location is defined. The resulting sample locations are uniformly distributed over the test area [11].

Cluster sampling selects samples of clusters and groups pixels within these clusters in order to reduce data collection costs. Even though pixels are grouped to clusters the reference classification needs to be performed for the spatial assessment unit defined in response design [12].

According to [10] **sample unit** is the fundamental unit of accuracy assessment that links spatial location on the map with a spatial location on the ground and represents the basis for map and reference data comparison. Sample unit can be a point, pixel, pixel block or a polygon.

For accuracy assessment to be statistically valid an adequate **number of samples** per class needs to be collected. According to [11] maps of 1 million acres surface and less than 12 classes require a minimum of 50 samples per class. A sample size of 75 to 100 is required for larger area maps. Additionally, [11] argues that the sample size needs to be selected based on practical considerations and should neither be too large nor too small. As presented in [14] the sample size in remote sensing is commonly calculated based on equation 1.

$$n \;=\; \frac{z^2_{\alpha/2}\; P(1\; - P)}{h^2}\,, \tag{1}$$

where h is the half width of the desired confidence interval, $z_{\alpha/2}$ is a critical value of the normal distribution for the two-tailed significance level α and P is the planning value for the population proportion. Since classification accuracy is often compared against a threshold target accuracy to fulfil pre-defined user's accuracy requirements equation 2

is used for determining the sample size in this case.

$$n = \frac{n'}{4}\left(1+\sqrt{1+\frac{2}{n'|P_1 - P_0|}}\right)^2, \tag{2}$$

where

$$n' = \left[\frac{z_\alpha\sqrt{P_0(1-P_0)}+z_\beta\sqrt{P_1(1-P_1)}}{P_1-P_0}\right]^2. \tag{3}$$

To calculate the sample size by equation 2 significance level α, the probability of making a Type II error β and minimum detectable effect size (a minimum meaningful difference in accuracy of classification accuracy P_1 and target accuracy P_0) need to be considered.

If the aim of classification accuracy assessment is comparison of classification accuracies and evaluation of statistical significance of proportion differences the equation 4 is used to determine the sample size. Equation 4 is used for independent samples [14].

$$n = \frac{n'}{4}\left(1+\sqrt{1+\frac{4}{n'|P_2 - P_1|}}\right)^2, \tag{4}$$

where

$$n' = \frac{(z_{\alpha/2}\sqrt{2\bar{P}\,\bar{Q}}+z_\beta\sqrt{P_1Q_1+P_2Q_2})^2}{(P_2-P_1)^2} \tag{5}$$

and $\bar{P}=\frac{P_1+P_2}{2}$ and $\bar{Q}=1-\bar{P}$. The total number of samples is $2n$.

2.3.2 Response design

Response design is a protocol by which the agreement of the map and reference data is defined. Response design specifies the source of reference data, the spatial assessment unit, the reference labelling protocol and the defining agreement [12].

In the response design the **source of reference data** collection is specified. It is important the reference data being of higher quality as the map data source and that its acquisition date matches the map data source acquisition date. If the high-quality reference data is not available, the same data source can be used for both map and reference classification under the condition that the reference classification process is more accurate. Ground visits, aerial photography, satellite imagery, lidar or forest inventory data are possible reference data sources for forest maps [12], [13].

Spatial unit at which map and reference data are compared is called **spatial assessment unit**. It is a unit at which the map was classified and reference data collected. Pixel, polygon or block of pixels can be selected as spatial assessment unit [12], [13].

Reference labelling protocol labels the information derived from reference data according to reference classification scheme. In this step, MMU for the reference classification needs to be specified. MMU represents the smallest labelled area in the reference data and can coincide with the spatial assessment unit but not necessarily [12], [13].

Rules for **defining agreement** are defined after performing map and reference classification and before conducting the accuracy assessment analysis. Based on defining agreement, labels of map and reference classification can match or not. The mapped category is correct if the labels match. If not, there is a misclassification. The defining agreement needs to be defined according to the type of reference and map classification scheme and homogeneous or heterogeneous assessment units [12], [13].

2.3.3 Analysis

The analysis is the third main component of accuracy assessment. In the analysis process numbers of matched and mismatched sample points are represented in the error matrix and the classification quality is quantified by the accuracy parameters. Additionally, the error matrix can be used to update area estimates of mapped categories. More details about the error matrix, accuracy parameters and the area estimation are given in the following three sections.

2.3.3.1 Error matrix

The main output of any accuracy assessment is the error matrix. Confusion matrix stores the number of correctly classified and misclassified sample points by comparing map and reference data. The number of rows and columns in the error matrix matches the number of classes on the map. While columns in the error matrix represent the reference data, rows show the map data. Reference data are assumed to be correct and the map data are being assessed. Correctly classified samples are located on the matrix diagonal. Misclassified sample points are located off-diagonal and therefore represent omitted and committed number of samples. The error matrix summarizes the agreement of map and reference data and is as such the key element for accuracy parameters estimation [11], [12]. Table 1 shows an example error matrix with q classes and its elements representing estimated area proportions p_{ij}.

		Reference				
		1	2	$\cdots$	q	
Map	1	p_{11}	p_{12}	$\cdots$	p_{1q}	p_{1+}
	2	p_{21}	p_{22}	$\cdots$	p_{2q}	p_{2+}
	$\vdots$	$\vdots$	$\vdots$	$\cdots$	$\vdots$	
	q	p_{q1}	p_{q2}	$\cdots$	p_{qq}	p_{q+}
		p_{+1}	p_{+2}	$\cdots$	p_{+q}	

Table 1: Error matrix for q classes

For simple random sampling, the estimated area proportions p_{ij} are calculated based on equation 6.

$$\hat{p}_{ij} \;=\; W_i \frac{n_{ij}}{n_{i+}}\,, \tag{6}$$

where W_i is the class i area proportion obtained from the map, n_{ij} is the number of sample points classified into class i on the map and class j in the reference data, n_{i+} is the total number of samples classified as class i on the map.

2.3.3.2 Accuracy parameters

Estimated area proportions $\hat{p}_{ij}$ reported in the error matrix are the basis to calculate overall accuracy, producer's accuracy, user's accuracy, omission error and commission error accuracy parameters.

Overall accuracy is the proportion of pixels correctly assigned to the map classes. It is calculated based on equation 7 as a sum of diagonal elements in the error matrix [11].

$$\hat{O} \;=\; \sum_{j=1}^{q} \hat{p}_{kk}\,, \tag{7}$$

Producer's accuracy is an individual accuracy measure of each class and it represents

the proportion of area that is the same class in the reference data and on the map [13], [11]. It is calculated based on equation 8.

$$\hat{P}_j \;=\; \hat{p}_{jj}/\hat{p}_j, \tag{8}$$

where $\hat{p}_j$ represents the true marginal proportions computed by summing estimated area proportions $\hat{p}_{ij}$ in each columns.

User's accuracy is as well a quality measure of individual class. User's accuracy is calculated from equation 9 by taking the number of correctly classified samples in class i from the diagonal and dividing it by the total number of samples classified as class i on the map. User's accuracy represents proportion of area classified into class i on the map that is the same class in the reference data [11], [13].

$$\hat{U}_i \;=\; n_{ii}/n_{i+}. \tag{9}$$

Omission error defines the proportion of pixels not assigned to the class they belong to. It is the probability that the area belonging to the class j in the reference data represents the same class in the map [13], [11].

$$\hat{p}_{kj}/\hat{p}_{+j}. \tag{10}$$

Commission error defines the proportion of pixels assigned to the class when they do not belong to that class. It is the probability that the area classified as the class i in the map represents the same class in the reference data [13], [11].

$$\hat{p}_{ik}/\hat{p}_{i+}. \tag{11}$$

According to [11], [13], [12] and [10] estimates of accuracy parameters need to be reported with their standard error. We can derive standard errors of accuracy measures and its confidence intervals from estimated variances. As described in [11], variances for simple random sampling scheme are calculated based on equation 12 for overall, 13 for producer's and 14 for user's accuracy.

$$V(\hat{O}) \;=\; \sum_{i=1}^{q} \hat{p}_{ii}(W_{i} - \hat{p}_{ii})/(W_{i}\, n)\,, \tag{12}$$

$$V(\hat{P}_{j}) \;=\; \hat{p}_{jj}\hat{p}_{j}^{-4}\left[\hat{p}_{jj}\sum_{j=1}^{q}\hat{p}_{ij}(W_{i} - \hat{p}_{ij})/(W_{i}n) + (W_{j} - \hat{p}_{jj})(\hat{p}_{j} - \hat{p}_{jj})^{2}/(W_{j}n)\right] \tag{13}$$

$$V(\hat{U}_{i}) \;=\; \hat{p}_{ii}(W_{i} - \hat{p}_{ii})/(W_{i}^{2}\, n)\,, \tag{14}$$

95 % confidence intervals for overall, producer's and user's accuracy are calculated from estimated variances based on equations 15.

$$\hat{O} \pm 1.96\sqrt{V(\hat{O})}\,, \quad \hat{P}_{j} \pm 1.96\sqrt{V(\hat{P}_{j})}\,, \quad \hat{U}_{i} \pm 1.96\sqrt{V(\hat{U}_{i})}\,, \tag{15}$$

where 1.96 is the value of z score for the corresponding 95% confidence interval.

2.3.3.3 Area estimation

Error matrix summarizes the number of misclassifications indicating disagreement of the map and the reference data. Therefore, the error matrix entries can be used to update area estimates of mapped categories and to determine their confidence inter-

vals [11]. Equations to estimate the adjusted forest/non-forest cover proportions and corresponding confidence intervals were presented by McRoberts in [15].

First, the naive estimator of forest proportion is calculated as:

$$\hat{\mu}_{F,naive} \;=\; \frac{1}{N}\left(\sum_{i=1}^{N}\hat{y}_i,\right), \tag{16}$$

where N is the total number of pixels in the map and $\hat{y}_i$ is mapped class. After, the bias of forest proportion estimator is determined by:

$$\hat{Bias}(\hat{\mu}_{F,naive}) \;=\; \frac{n_{01}-n_{10}}{n}, \tag{17}$$

where n_{01} represent the number of misclassified forest samples on the map, n_{10} is the number of non-forest samples incorrectly classified on the map and n is the total number of sample points. Forest proportion is then calculated by subtracting the bias from the naive forest proportion estimator:

$$\hat{\mu}_{F} \;=\; \hat{\mu}_{F,naive} - \hat{Bias}(\hat{\mu}_{F,naive}), \tag{18}$$

The variance of adjusted forest proportion is determined by:

$$\hat{Var}(\hat{\mu}_{F}) \;=\; \frac{1}{n-1}\left[(1-V(\hat{O})) - \hat{Bias}(\hat{\mu}_{F,naive})^2\right], \tag{19}$$

where $V(\hat{O})$ is the overall accuracy obtained from the error matrix.

To quantify the accuracy of forest cover maps the 3 main components; the sampling design, the response design and the analysis of the accuracy assessment protocol need to be defined. The accuracy assessment protocols determined for generated forest cover maps

are explained in more detail in chapter 4.3 taking into account the accuracy assessment foundations explained in this chapter.

3 TEST AREAS AND DATA

3.1 Test areas

Conspicuous reduction in forest stand areas are the main reason for developing countries to undertake REDD+ activities. The most extensive deforestation and forest degradation occur in the tropical forest. Therefore, two distinct tropical forest regions, one in Peru and another in Ethiopia were selected to analyse the effect of MMU, pixel size and spectral resolution on the accuracy of forest maps. Test areas are shown in Figure 2.

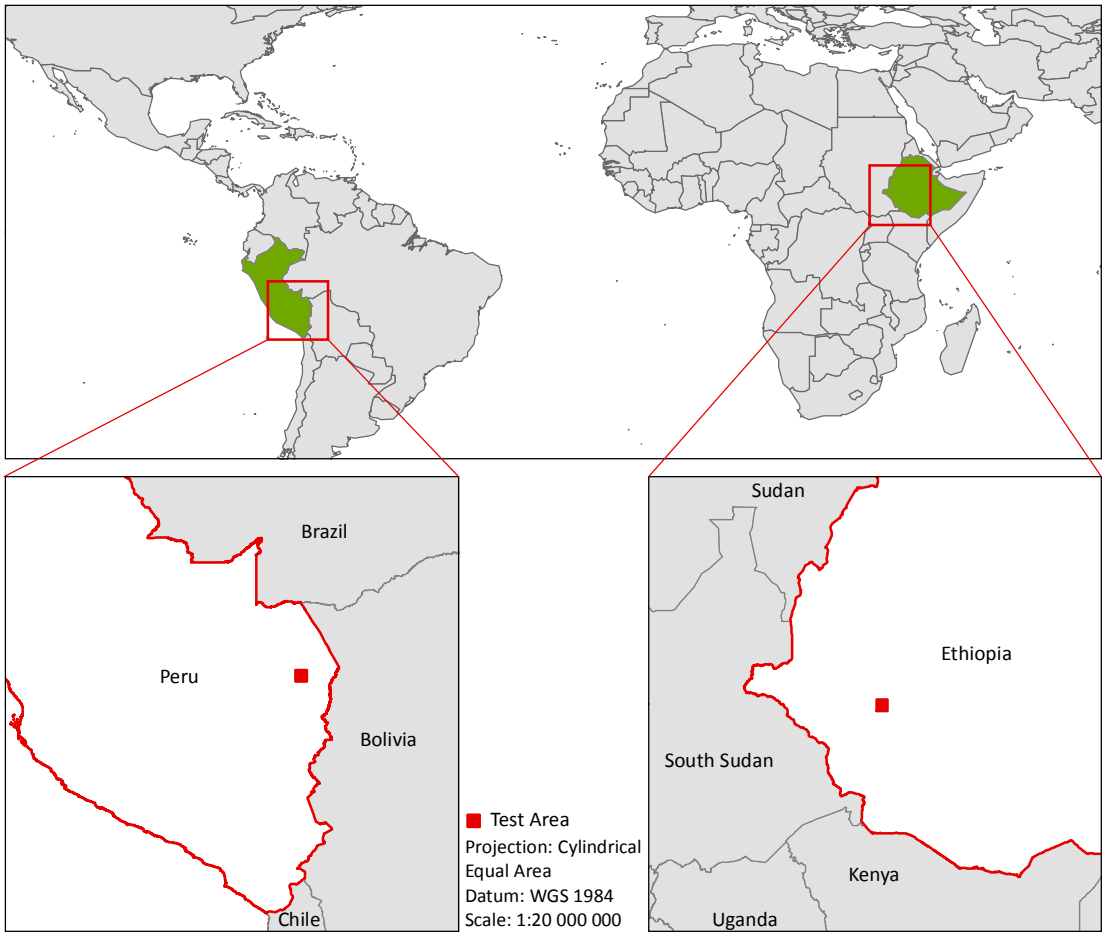

Figure 2: Accuracy assessment test areas

The exact test sites for this Master's thesis were selected from demonstration areas used in the ForMoSa project. Demonstration areas were determined based on the SPOT-5/Take5 image takes which used SPOT-5 satellite sensor to simulate Sentinel-2 mission image time series over 150 sites from April to September 2015 [16]. From selected demonstration areas subsets matching the extent of one RapidEye tile per area were selected. The main criteria for selecting the tiles were acceptable cloud cover and data availability.

The first test area is located in Madre de Dios region in Peru. It encompasses the area of one selected RapidEye image tile which is 62500 ha. The test site is located west of Puerto Maldonado, the capital of Madre de Dios region along the Inter-Oceanic highway and Madre de Dios river. The regional climate is tropical monsoon with a dry period from June to August and annual precipitation from 1600 to 2400 mm [17]. Main types of vegetation in the area are semi-deciduous dense forest on plains, semi-deciduous dense forest on hills and mixed bamboo or scattered trees on plains [17]. According to [17] deforestation prevails near roads, rivers and towns and is mainly caused by small-scale cattle ranching, mixed small-scale agriculture and cattle ranching, mining, subsistence agriculture and human settlements. Forest degradation is driven by multiple-scale timber harvesting.

The second test area is located at the border of Kaffa and Jimma administrative zones in Ethiopia and also covers an area of 62500 ha. Kaffa zone belongs to Southern Nations, Nationalities and People's region (SNNPR) and Jimma zone to Oromia region. The test site is located around 60 km southwest from Jimma, the largest city of Oromia region. The southern part of the test area is a part of Kaffa Biosphere Reserve. The area is located in Ethiopian highlands and most of the test site is located more than 1400 m above sea level. The climate is tropical with the wet season between March and October. According to [18] high forest and high woodland forest types are estimated to be the

highest within Oromia and SNNPR regions. The main drivers of deforestation and forest degradation in Ethiopia include large-scale agriculture, extraction of wood for charcoal and firewood, overgrazing and forest fires.

3.2 Data

In order to answer the research questions and meet the research objectives satellite imagery of high- and medium- resolution is necessary. To test the effect of different satellite sensor resolutions on the accuracy of forest cover mapping high-resolution RapidEye and medium-resolution Landsat-8 and Sentinel-2 images were used. The RapidEye imagery was selected because its fine resolution enables discrimination of single trees and small groups of trees on a single pixel level. Therefore, the presence of mixed pixels in high-resolution imagery is diminished and forest cover maps can be generated using clear forest definition. In contrast to RapidEye imagery, Landsat-8 and Sentinel-2 sensors have a good spectral resolution which can be used to reduce the mixed pixel problem and possibly produce forest cover maps of high accuracy.

RapidEye satellite system is a constellation of five high-resolution satellites with five spectral bands (blue, green, red, red edge and near-infrared), 6.5 m spatial resolution which is resampled to 5 m pixel size during orthorectification. For processing and analysis level 3A RapidEye Ortho product was used. The RapidEye Ortho product is available as 25 by 25 kilometre tile. Level 3A imagery is projected to Universal Transverse Mercator (UTM) cartographic projection, corrected for terrain distortions and as such having accurate geo-location.

Landsat-8 Operational Land Imager (OLI) collects data in nine spectral bands in the range of 0.43 µm-1.38 µm. On board Landsat-8 additional Thermal Infrared Sensor (TIRS) acquires imagery in the range of 10.6 µm- 12.51 µm. The pixel size of OLI multispectral and TIRS bands is 30 m, besides OLI panchromatic band has a pixel size

of 15 m. Imagery collected for the thesis test sites is terrain corrected (Level 1T) and projected to UTM cartographic projection.

Sentinel-2 carries the Multispectral Instrument (MSI) acquiring imagery in 13 spectral bands at 10 m, 20 m and 60 m spatial resolution in the range of 0.443 µm-2.19 µm. Product used for the analysis is Level 1C product which is radiometrically and geometrically corrected. Top-of-atmosphere reflectances (ToA) of Level-1C product are projected to UTM cartographic projection. The three used satellite specifications are presented in Table 2 and the acquisition details for each satellite sensor and test site in Table 3.

Satellite	Spatial resolution	Number of spectral bands	Processing level
RapidEye	5 m	5	3A
Landsat-8	30 m	11	1T
Sentinel-2	10 m	13	1C

Table 2: Satellite specifications

Satellite	Test area	Acquisition date
RapidEye	Ethiopia	2016-01-09
Landsat-8	Ethiopia	2016-03-10
Sentinel-2	Ethiopia	2016-03-28
RapidEye	Peru	2016-07-20
Landsat-8	Peru	2016-08-24
Sentinel-2	Peru	2016-08-15

Table 3: Acquisition information

4 FOREST COVER MAPPING AND ACCURACY ASSESSMENT

This chapter presents the methodology used to generate forest cover maps from high- and medium-resolution satellite imagery and describes designed tests to assess the accuracy of derived forest cover maps.

4.1 Image pre-processing

To enable a visual comparison of forest cover maps generated from RapidEye, Landsat-8 and Sentinel-2 imagery, images were co-registered to RapidEye reference images. RapidEye and Landsat-8 images were automatically co-registered using a Python software script with implemented PCI Geomatics co-registration routine developed at Planet. Sentinel-2 images were manually co-registered in PCI Geomatics software to the same RapidEye reference images. Atmospheric correction using ATCOR IDL 8.4 was applied to RapidEye images to turn the radiance values into surface reflectance values. Due to the presence of haze in some areas of the image, haze reduction was applied to RapidEye and Landsat-8 data using ATCOR PCI Geomatics tool. Additionally, Landsat-8 and Sentinel-2 images were clipped to the extent of RapidEye tiles.

4.2 Forest cover mapping for REDD+ MRV

Forest cover for REDD+ MRV is mapped based on a certain forest definition. Forest definition parameters are crucial for mapping forest and can vary among countries participating in REDD+. Common threshold parameters used in forest definition are minimum forest area, in this thesis referred to as MMU, minimum height of forest stands and minimum tree crown cover [2]. As described in 3.1 for this Master's thesis, areas in

Ethiopia and Peru were used to test the accuracy of forest cover maps. Ethiopia adopted national forest definition with threshold parameters of at least 20% tree cover canopy over a minimum area of 0.5 ha covered by trees and bamboo, attaining a height of at least 2 m [19]. In Peru, the MMU of 0.09 ha, 5 m minimum tree height at maturity in situ and canopy cover of at least 10% are the threshold parameters of forest definition [20].

In this study, forest cover was mapped based on different satellite sensor resolution imagery listed in 3.2. To analyse the effect of high and medium satellite sensor resolutions on forest map accuracy, forest cover maps were generated at the highest resolution possible for each satellite sensor. Therefore, only the crown cover percent threshold parameter specified by the national forest definition was applied in the forest mapping process to the two areas respectively. Different methodologies based on Asner and Magdon described in 2.1 were used to map forest from high- and medium-resolution satellite imagery and are described in the following sections.

4.2.1 Forest cover mapping from high-resolution satellite imagery

A high level of detail can be recognized from fine resolution satellite imagery. If the size of the object on the ground is approximately the size of the image pixel and if the pixel contains only one land cover type, this pixel is spectrally pure [21]. 5 m spatial resolution RapidEye imagery discriminates and maps single big tree canopies and small tree groups. Connected chunks of single trees and small groups of trees can then be mapped as forest considering forest definition crown cover threshold. Therefore, the forest cover mapping from high-resolution satellite imagery is divided into two steps: the tree cover mapping and the forest cover mapping. The entire mapping workflow presented in [22] is shown in Figure 3. The accuracy assessment process is also included in the workflow.

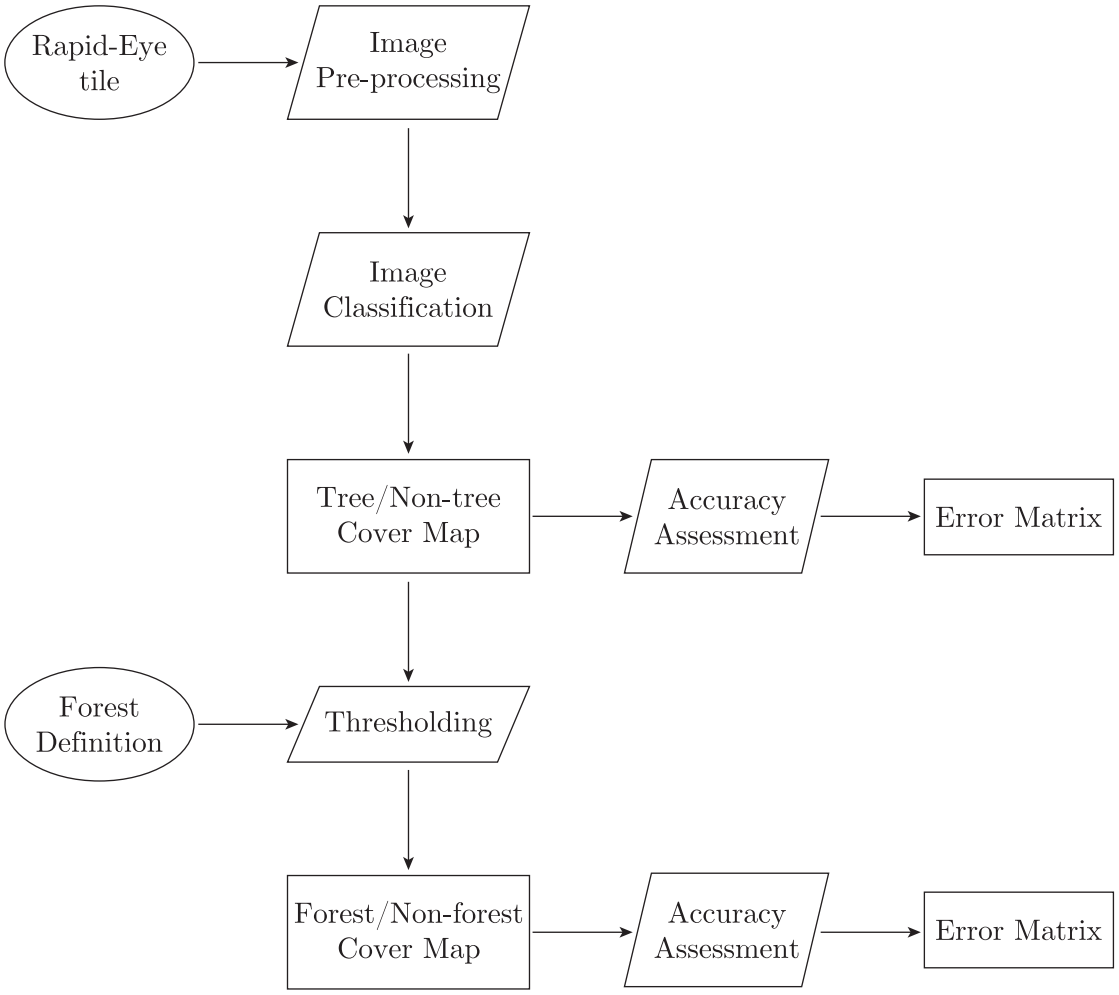

Figure 3: Forest cover mapping workflow for high-resolution imagery

4.2.1.1 Tree cover map

On the tree cover map, two classes: tree and non-tree are mapped. For these two classes, training samples were collected from the original RapidEye satellite image. When needed, a cloud mask layer was created manually. The training samples were collected by visually identifying areas of dark, dense forest or individual trees and groups of trees with the aim to sample only unambiguous, pure pixels, to a tree or non-tree category and let the classification algorithm decide how to classify problematic i.e. spectrally impure

pixels. The training samples were used to train the Classification and Regression Tree (CART) decision algorithm which classified each RapidEye pixel as tree or non-tree. The classification was performed by a Python-based software implementation of Breiman's CART algorithm described in [23] and developed at Planet. For each test site, few classification iterations using different training samples were made in order to improve the output tree cover map. At the end of each iteration, resulting maps were visually examined for misclassifications. The tree cover map with the least classification errors as assessed visually was selected as the final classification tree cover map of the test area.

4.2.1.2 Forest cover map

In order to produce the forest cover map, forest crown cover threshold criteria needs to be applied to the remote sensing data. The thematic tree cover layer generated was used as a reference to which minimum area and a minimum level of crown cover thresholds were applied. It was assumed that all pixels classified as trees represented trees above the minimum height defined by the forest definition. In the process of creating the forest cover map, the individual tree/non-tree cover pixels were grouped into larger spatial units according to the target MMU of the forest cover map. The target MMU included a number of tree and non-tree cover pixels and was classified as forest based on the percent tree cover threshold parameter determined by the national forest definition. In practical terms, the MMU was represented by squared grid cells overlaying the tree cover map. Thresholding was done with a software script developed at Planet which counts the number of tree cover pixels inside the grid cell and divides it by the total number of pixels in a grid cell. This is how the percent of trees in a grid cell was calculated. Percentage of tree cover pixels represents the canopy cover percentage over a minimum area (MMU) which in our case coincides with the grid cell size. Finally, the grid cell was assigned a forest class if the percentage was above the minimum level of crown cover and the non-forest attribute category if the percentage was under it. The final output was

a binary forest cover map with two classes: forest and non-forest, generated according to crown cover density values. The process of thresholding the tree cover map based on grid cells is shown in Figure 4. Different sizes of MMUs represented by corresponding grid cell sizes were then used to test the effect of MMU on the accuracy of forest cover maps.

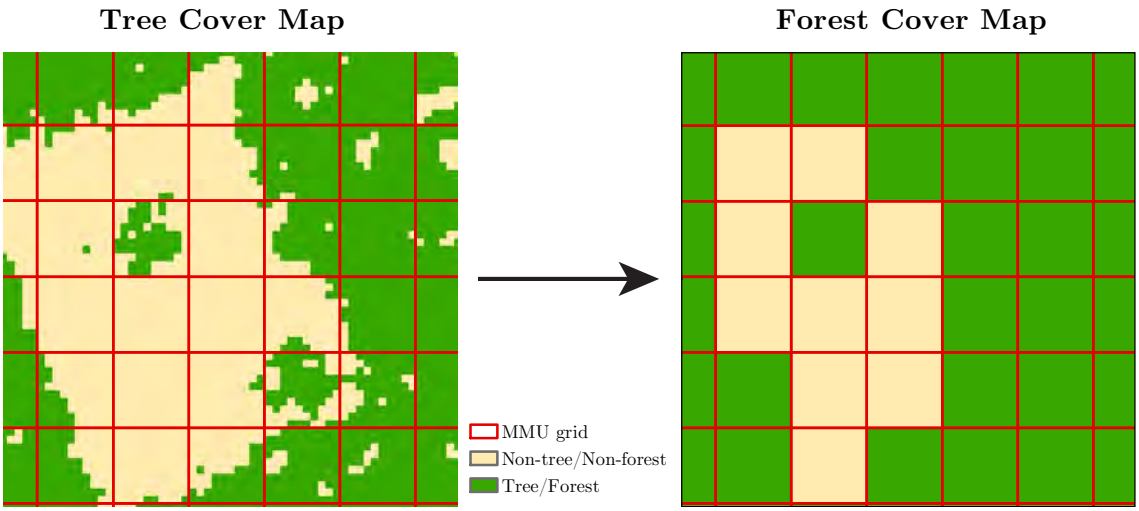

Figure 4: Tree and forest cover maps overlaid with the MMU grid

4.2.2 Forest cover mapping from medium-resolution satellite imagery

Spatial resolution limits the level of detail represented in the satellite image. Spectral signatures from small size features are combined with other reflecting materials spectra into satellite-observed spectral responses. Consequently, a mixture of several distinct materials, called endmembers can occur in a single image pixel [21]. In contrast to high-resolution satellite imagery, single tree canopies and groups of small trees cannot be recognized from a single pixel in a medium-resolution satellite imagery. However, it is possible to define the fraction of tree endmember in one pixel using sub-pixel analysis techniques. The fraction of tree endmember defines the canopy cover percent in each

pixel and can be thresholded based on forest definition to assign pixels forest or non-forest attribute category. The forest cover mapping workflow is shown in Figure 5.

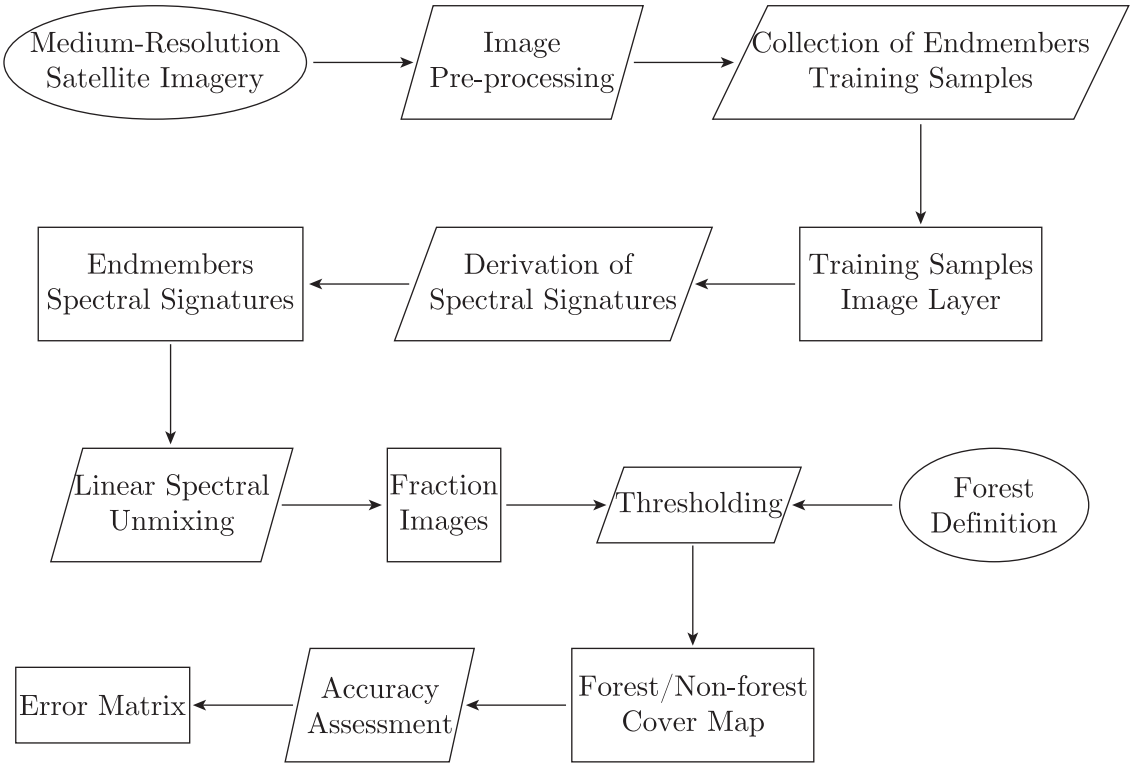

Figure 5: Forest cover mapping workflow for medium-resolution imagery

4.2.2.1 Spectral unmixing

Spectral mixing analysis (SMA) also referred to as spectral unmixing is a sub-pixel classification technique which optimally estimates the fraction of each endmember spectra in all image pixels [24]. To obtain fractions endmembers for test areas medium-resolution imagery, the linear spectral unmixing analysis was performed in PCI Geomatics software.

The linear spectral unmixing analysis was divided into two steps:

- Generation of endmembers spectral signatures using the CSG2 function.

- Generation of fraction images applying UNMIX function.

Spectral signatures were derived from selected image channels based on collected training areas. Only spectrally pure pixels should be included in training areas. CSG2 function stores numerous statistical parameters in derived spectral signature file which represent an input into UNMIX function [25]. UNMIX algorithm uses linear mixture model of the following form:

$$\boldsymbol{d} \;=\; R\;\boldsymbol{f}\,. \tag{20}$$

Elements of matrix 21 with $m \times n$ dimension represent the spectral reflectance of n endmembers in m bands. For linear spectral unmixing to be successful, the number of endmembers should not exceed the number of spectral bands [26].

$$R = \begin{bmatrix} r_{11} & r_{12} & \cdots & r_{1n} \\ r_{21} & r_{22} & \cdots & r_{2n} \\ \vdots & \vdots & \vdots & \vdots \\ r_{m1} & r_{m2} & \cdots & r_{mn} \end{bmatrix} \tag{21}$$

All n endmembers fractions are represented in the $\boldsymbol{f}$ vector:

$$\boldsymbol{f} = \begin{bmatrix} f_1 \\ f_2 \\ \vdots \\ f_m \end{bmatrix} \tag{22}$$

Linear mixing model represents pixel spectral reflectance measured by the satellite sensor as a sum of endmembers reflectance values multiplied by fractions for each spectral band as shown in equation 23.

$$\boldsymbol{d} = \begin{bmatrix} r_{11}\ f_1 + r_{12}\ f_2 + \cdots + r_{1n}\ f_m \\ r_{21}\ f_1 + r_{22}\ f_2 + \cdots + r_{2n}\ f_m \\ \vdots \\ r_{m1}\ f_1 + r_{m2}\ f_2 + \cdots + r_{mn}\ f_m \end{bmatrix} \tag{23}$$

The following two constraints should be considered in the linear mixing model:

$$\begin{aligned} 0 \leq f_m \leq 1 \\ f_1 + f_2 + ... + f_m \ = \ 1 \end{aligned} \tag{24}$$

Least squares singular value decomposition method is used to obtain adjusted endmember fractions for each pixel. The final output of UNMIX algorithm are fraction images for each endmember containing the endmember fractions in each image pixel [26].

4.3 Forest cover maps accuracy assessment

To ensure sufficient accuracy of processed datasets for REDD+ MRV, the quality of resulting maps needs to be quantified by performing accuracy assessment. Thematic accuracy of forest cover maps is quantified by constructing an error matrix and calculating accuracy parameters by following project specific design steps of accuracy assessment.

Three accuracy assessment tests were designed in order to provide answers to research questions in 1.3. First, the accuracy test was designed to assess the effect of image spatial

resolution on the accuracy of forest cover maps. The second accuracy test was designed to quantify the impact of chosen MMU on the accuracy of derived forest cover maps. Additionally, a separate accuracy test was designed to quantify tree cover maps accuracies. All tests were designed according to good practice recommendations described in 2.3. The three accuracy tests are presented in more detail in the next sections.

4.3.1 Accuracy test of forest maps derived from high- and medium-resolution imagery

Forest cover maps processed from RapidEye, Landsat-8 and Sentinel-2 satellite sensors were tested to quantify the effect of the image resolution on the accuracy of forest cover maps. Accuracy assessment was performed for the two test sites described in 3.1 on forest cover maps produced as presented in 4.2.1 for high-resolution satellite imagery and 4.2.2 for medium-resolution satellite imagery. Forest cover maps generated at the highest resolution possible for each satellite sensor were assessed for accuracy. The overview of accuracy assessment inputs is given in Table 4.

Test area	Satellite	Forest cover map MMU	Forest cover mapping method
Ethiopia & Peru	RapidEye	15 m x 15 m	4.2.1
Ethiopia & Peru	Landsat-8	30 m x 30 m	4.2.2
Ethiopia & Peru	Sentinel-2	10 m x 10 m	4.2.2

Table 4: List of forest cover maps that were assessed for accuracy

Each of forest and non-forest classes cover approximately 50% of the area mapped on derived forest cover map of Ethiopia which was generated from high-resolution satellite imagery. The forest cover map of Peru derived from high-resolution satellite imagery includes approximately 80% forest and 20% non-forest cover. As the smallest mapped area represents 20% of the map there are no classes that occupy a very small proportion

of area on the map. Due to the simple classification scheme of forest cover map, it is unlikely that any map category would be under-sampled. Therefore, the simple random sampling approach was used to select samples from the map. Additionally, good statistical properties of simple random sampling scheme enable unbiased selection of samples. Since ground reference data were not available for examined test sites, very high-resolution Google Earth satellite imagery was used as reference data source. Consequently, a collection of samples is not limited to the physically accessible reference sites. Therefore, usage of simple random sampling as the probability sampling design scheme is favourable for the accuracy assessment of generated forest cover maps. The sampling unit for the image resolution accuracy test corresponded the MMU applied for the forest cover mapping and matched forest cover map resolutions specified in Table 4.

In remote sensing, classification accuracy output is typically compared to some threshold target accuracy. In this case, the threshold was set to the minimum acceptable accuracy of 85%. Therefore, the number of sample units was calculated based on equation 2 presented in section 2.3.1. According to sample size calculation, 302 samples needed to be picked from each forest cover map by simple random sampling approach. Sample points falling into the image area covered by clouds were excluded from the accuracy assessment. The least, 66 out of overall 302 samples fell in the forest class for Peru forest cover map generated from medium-resolution Sentinel-2 imagery. Despite the relatively small sample size collected for the forest class, this category was not underrepresented in the sampling process as the number of obtained samples was more than 50.

Acquisition dates of very-high-resolution Google Earth reference satellite imagery are specified in Table 5. The spatial assessment unit coincided with the MMU and was a block of 3 by 3 pixels (15 m by 15 m) for RapidEye, 30 m by 30 m pixel for Landsat-8 and 10 m by 10 m pixel for Sentinel-2. Thus, spatial assessment units matched spatial units used in sampling design. The reference classification scheme was identical with the map

classification scheme and was composed of forest and non-forest categories. Reference data was labelled as forest or non-forest according to accepted crown cover threshold parameters for Ethiopia and Peru. All above mentioned components of response design protocol are listed in Table 6.

Test area	Reference datasource	Acquisition date of reference data
Ethiopia	Google Earth	end of 2014, 19.12.2014, 10.11.2014
Peru	Google Earth	3.9.2011, 28.7.2013, 26.9.2013, 9.9.2010

Table 5: Reference data acquisition dates

Test area	Satellite	Reference datasource	Spatial assessment unit	MMU	Reference classification scheme
Ethiopia & Peru	RapidEye	Google Earth	15 m	15 m	Forest; Non-forest
Ethiopia & Peru	Landsat-8	Google Earth	30 m	30 m	Forest; Non-forest
Ethiopia & Peru	Sentinel-2	Google Earth	10 m	10 m	Forest; Non-forest

Table 6: Components of response design protocol

Classification of reference data was based on dot-grid sampling technique which uses square sample plots containing equally spaced point grid. The point grid overlaying reference data enables estimation of the canopy cover percent defined as the ratio of grid points intersecting tree canopies and the total number of grid points in the sample plot [27], [13] and is shown in Figure 6. The size of the dot-grid sample plot matched the spatial assessment unit.

Figure 6: Dot-grid sampling technique implemented in Google Earth for Landsat-8 forest cover map verification

After all the steps of the sample and response design were defined and implemented the accuracy assessment analysis was conducted. The main output of the accuracy assessment was the error matrix and the accuracy parameters derived from the error matrix. First, the error matrices of the forest cover maps generated from RapidEye, Landsat-8 and Sentinel-2 were created. The error matrices report the number of correctly classified and misclassified samples recognised by the defining agreement according to the reference labelling protocol. As described in 2.3.3.1 section, it is preferable the error matrices to be reported in terms of proportions p_{ij}. To enable comparison of error matrices they were standardised by introducing conditional probabilities based on column marginal proportions p_{j}. Standardisation was characterized with column conditional probabilities summing to 1 [10]. Next, the accuracy parameters: overall, producer's and user's accuracy for the three forest cover maps were calculated as presented in 2.3.3.2 section. All

accuracy parameters were reported with their corresponding 95% confidence intervals calculated based on equations shown in 2.3.3.2 section. These accuracy parameters can then be used to compare the accuracy of forest cover maps generated from different satellite imagery resolutions. Additionally, mapped area proportions were updated for bias considering the number of misclassified samples for forest and non-forest categories as described in 2.3.3.3. Adjusted class area proportions were reported with corresponding confidence intervals and compared to mapped area proportions.

4.3.2 Tree cover map accuracy test

When using high-resolution RapidEye satellite imagery as the data source for forest cover mapping, an intermediate tree cover map layer needs to be created. Based on this tree cover map, the forest cover maps are processed following the methodology described in 4.2.1.2. Since the tree cover map forms the basis for the forest cover mapping its quality was of particular interest. Therefore, the tree cover maps of test sites in Peru and Ethiopia were assessed for accuracy by conducting a separate accuracy test. The overview of accuracy assessment input data is given in Table 7.

Test area	Satellite	Forest cover map MMU [m]	Forest cover map MMU [pixels]	Forest cover mapping method
Ethiopia	RapidEye	5 x 5	1 x 1	4.2.1.1
Peru	RapidEye	5 x 5	1 x 1	4.2.1.1

Table 7: List of tree cover maps assessed for accuracy

The simple random sampling protocol was selected for the tree cover maps accuracy assessment, mainly because of the reasons already described in 4.3.1. The same number of sample points was used as in the Image resolution forest map accuracy test. A point sampling unit with a buffer of 10 m was used to link the locations in the map and on the ground. The 10 m buffer was created to compensate for the positional accuracy error

and at the same time ensure the inclusion of the whole 5 by 5 m pixel in the accuracy assessment sample area.

The same as in the Image resolution forest map accuracy test, very-high-resolution Google Earth satellite imagery was used as a reference data source. Acquisition dates for Google Earth imagery are given in Table 5. The tree cover map and the reference imagery were compared on a polygon level. Polygons were defined by taking sample points as an origin for constructing the 10 m buffer around each sample point. The reference and map classification schemes both included tree and non-tree categories. These categories were compared and marked as a match if more than 50 % of the polygon area was covered by the tree canopy and as a mismatch if less than 50 % of the polygon area represented the tree crown.

In the analysis process, the number of mismatches and matches in each classification category was summarized in the error matrix. Then, the standard set of accuracy parameters was calculated as described in 2.3.3.2 and 4.3.1 sections. The accuracy parameters reported with their 95 % confidence intervals represent the final output of the tree cover accuracy analysis test and quantify the classification accuracy of the tree cover maps.

4.3.3 Minimum mapping unit forest map accuracy test

To assess the effect of MMU on the accuracy of forest cover maps, a set of different forest cover maps created based on various MMUs from high-resolution RapidEye satellite imagery are tested for accuracy. Forest cover maps for the two test sites described in 3.1 were assessed for accuracy. All forest cover maps were generated from high-resolution satellite imagery based on the methodology described in 4.2.1.2. The overview of accuracy assessed MMUs is given in Table 8.

The forest cover maps produced for different MMUs contain two mapped categories:

forest and non-forest. Each of these two map classes cover a considerably large area of the forest cover map. Since none of the classes encompass a small map area and the classification scheme is binary, the simple random sampling was used to distribute samples in the map. The aim of Minimum mapping unit forest map accuracy test is to detect differences in accuracy of different forest cover map resolutions with respect to the highest map resolution possible, the tree cover map. In this way, the focus is exclusively on the effect of spatial generalisation and therefore the forest cover maps were compared on the point level. As classification accuracies of forest cover maps need to be compared the required number of samples for rigorous accuracy assessment was calculated using equation 4 presented in section 2.3.1. Based on the calculations the required number of samples for the accuracy assessment was 1449.

Test area	Satellite	Forest cover map MMU [m]	Forest cover map MMU [pixels]
Ethiopia & Peru	RapidEye	15 x 15	3 x 3
		30 x 30	6 x 6
		50 x 50	10 x 10
		70 x 70	14 x 14
		100 x 100	20 x 20
		150 x 150	30 x 30
		200 x 200	40 x 40
		250 x 250	50 x 50
		300 x 300	60 x 60

Table 8: List of forest cover maps assessed for accuracy

In this accuracy test, all forest cover maps are compared to the highest resolution map derived from the original data source. Therefore, the high-resolution tree cover map was used as a reference for the accuracy assessment. The forest cover maps derived for MMUs specified in Table 8 were assessed against the reference tree cover map based on the point sample unit. If the sample point in the tree cover map represents a tree and the same point is classified as forest in the forest cover map, the forest cover map

classification was correct, if not the classification was incorrect. Correspondingly, if the sample point represented non-forest in the forest map and non-tree in the reference data, the labels match, if not a misclassification occurred.

The results of agreement between reference and map data are summarized in the error matrix. For each MMU for both test sites in Peru and Ethiopia accuracy parameters were calculated from the corresponding error matrix. Overall, user's and producer's accuracies were calculated based on equations presented in 2.3.3.2 and were reported with the 95 % confidence intervals. To obtain statistically rigorous results, accuracy assessment of each test site was performed for 5 independent iterations. Therefore, the accuracy assessment was based on 5 different random distributions of sample points. It is important to note that in this test the emphasis is on the differences in accuracy of degraded MMU respect to the highest MMU possible (tree cover). In this way, we can focus exclusively on the effect of spatial generalization.

In this chapter methodologies for mapping forest cover from high- and medium-resolution satellite data, tree cover mapping and corresponding tests to quantify the accuracy of forest cover maps generated from different satellite imagery resolutions and MMUs were described in detail. In the following 4 chapter the results of presented accuracy tests are presented.

5 RESULTS AND DISCUSSION

Results in this chapter are presented in the same sequence as accuracy tests. First, the Image resolution forest map accuracy test results are presented and discussed, followed by the Tree cover map and Minimum mapping unit forest cover accuracy test results and discussion.

5.1 Accuracy test of forest maps derived from high- and medium-resolution imagery

Accuracies of forest cover maps generated from different satellite sensors image resolutions quantify the effect of mixed pixels in medium-resolution imagery with respect to high-resolution imagery. Error matrices for the six forest cover maps generated were reported in terms of proportions $\hat{p}_{ij}$ in Tables 21 - 23 included in Appendix. Accuracy parameters are reported with corresponding 95% confidence intervals for both test sites in Tables 9 - 12.

Obvious differences in generated forest cover maps from RapidEye, Sentinel-2 and Landsat-8 for Peru test site could be visually observed (Figure 7). Overall accuracies in Table 9 for Peru test site show overall accuracy differences of forest cover maps generated from Sentinel-2 (52.63% ± 4.70%), Landsat-8 (78.25% ± 4.06%) and RapidEye (95.56% ± 2.31%) imagery.

Satellite sensor	Overall accuracy
RapidEye	95.56% ± 2.31%
Sentinel-2	52.63% ± 4.70%
Landsat-8	78.25% ± 4.06%

Table 9: Overall accuracies with confidence intervals for Peru forest maps

35.98% ± 5.39% was the user's accuracy for the non-forest category of the forest cover map processed from Sentinel-2 data. Significantly different, 53.13% ± 5.60% user's accuracy of the non-forest category was obtained from the forest cover map generated from Landsat-8 imagery and 98.61% ± 1.32% from RapidEye imagery. On the contrary, comparable producer's accuracies for the non-forest category were obtained for all three analysed forest cover maps. The main reason for high producer's and low user's accuracies for a non-forest class in the case of Sentinel-2 and Landsat-8 imagery could be the overestimated non-forest area in both forest maps. For all three sensors, higher user's accuracies for the forest category were observed. In comparison, lower, 36.26% ± 2.44% forest class producer's accuracies occurred for Sentinel-2 and 76.40% ± 3.55% for Landsat-8 based forest cover maps. In the case of low forest producer's accuracies, not sufficient area was labelled forest on the map when compared to the reference data. Individual categories accuracy parameters for Peru are reported in Table 10.

Satellite sensor	Producer's accuracy Forest	Producer's accuracy Non-forest	User's accuracy Forest	User's accuracy Non-forest
RapidEye	99.64% ± 0.77%	82.51% ± 7.77%	94.81& ± 2.50%	98.61% ± 1.32%
Sentinel-2	36.26% ± 2.44%	96.93% ± 3.65%	96.97% ± 1.92%	35.98% ± 5.39%
Landsat-8	76.40% ± 3.55%	84.09% ± 7.76%	93.79% ± 2.71%	53.13% ± 5.60%

Table 10: Accuracy parameters with confidence intervals for Peru forest maps

On the contrary, overall accuracies reported in Table 11 for the test site in Ethiopia are relatively high comparing to the ones reported for Peru. Nevertheless, an evident drop in overall accuracy occurs for forest cover maps generated from medium-resolution satellite imagery. Overall accuracies of 94.72% ± 2.52% for RapidEye, 87.00% ± 3.80% for Sentinel-2 and 86.77% ± 3.66% for Landsat-8 based forest cover maps were obtained.

Satellie sensor	Overall accuracy
RapidEye	94.72% ± 2.52%
Sentinel-2	87.00% ± 3.80%
Landsat-8	86.77% ± 3.66%

Table 11: Overall accuracies with confidence intervals for Ethiopia forest maps

As can be seen from Table 12 high producer's and user's accuracies for Ethiopian forest cover map derived from RapidEye imagery verify correct classification of most image pixels. The accuracy of individual category accuracy parameters decreased for Sentinel-2 and Landsat-8 based forest maps. 78.41% ± 4.64% user's accuracy for non-forest class and 76.60% ± 5.07% producer's accuracy for forest category were obtained for forest maps generated based on Landsat-8 imagery. In comparison, 98.41% ± 1.41% user's forest class accuracy and 98.57% ± 1.94% producer's non-forest category accuracy were assessed. Identically as for Peru forest cover maps, low non-forest class user's accuracy shows high disagreement between mapped non-forest and what is considered non-forest based on the reference data. Low producer's accuracy of the forest category demonstrates insufficient area labelled as forest on the map comparing to reference data.

Test area	Producer's accuracy Forest	Producer's accuracy Non-forest	User's accuracy Forest	User's accuracy Non-forest
RapidEye	96.07% ± 2.94%	93.28% ± 3.79%	93.79% ± 2.72%	95.74% ± 2.28%
Sentinel-2	85.27% ± 4.91%	88.72% ± 4.52%	88.28% ± 3.64%	85.81% ± 3.95%
Landsat-8	76.60%± 5.07%	98.57% ± 1.94%	98.41% ± 1.41%	78.41% ± 4.64%

Table 12: Accuracy parameters with confidence intervals for Ethiopia forest maps

Accuracy assessment results show high and stable accuracy measures for high-resolution RapidEye imagery. Derived accuracy parameters do not differ significantly regarding the test site or mapped category. However, accuracies differ considerably depending on the test site when forest cover maps were generated from medium-resolution satellite im-

agery. The most pronounced differences in overall, forest class producer's and non-forest class user's accuracies were observed for Sentinel-2 medium-resolution satellite imagery. Results of the image resolution accuracy test show that lower sensor image resolutions decrease the overall, producer's and user's accuracy of forest cover mapping. This effect is more obvious in the case of Ethiopia where the accuracy parameters decrease with respect to decreasing sensor spatial resolution. Moreover, the spectral unmixing method used to map forest from medium-resolution satellite imagery was significantly less accurate than the forest mapping from high-resolution satellite data. Especially in the case of Peru for Sentinel-2 based forest map, the sub-pixel classification technique failed to estimate fractions of endmembers accurately. One reason for lower accuracy of medium-resolution satellite imagery based forest cover maps might be small tree endmember fractions sub-pixel classification technique needs to extract. Lower overall accuracies for Peru test site where the crown cover threshold was 10% in comparison to Ethiopia test site 20% threshold could confirm spectral unmixing methodology being less accurate for smaller tree cover thresholds. Generated foreset cover maps for test sites in Peru and Ethiopia are shown in Figure 7 and 8.

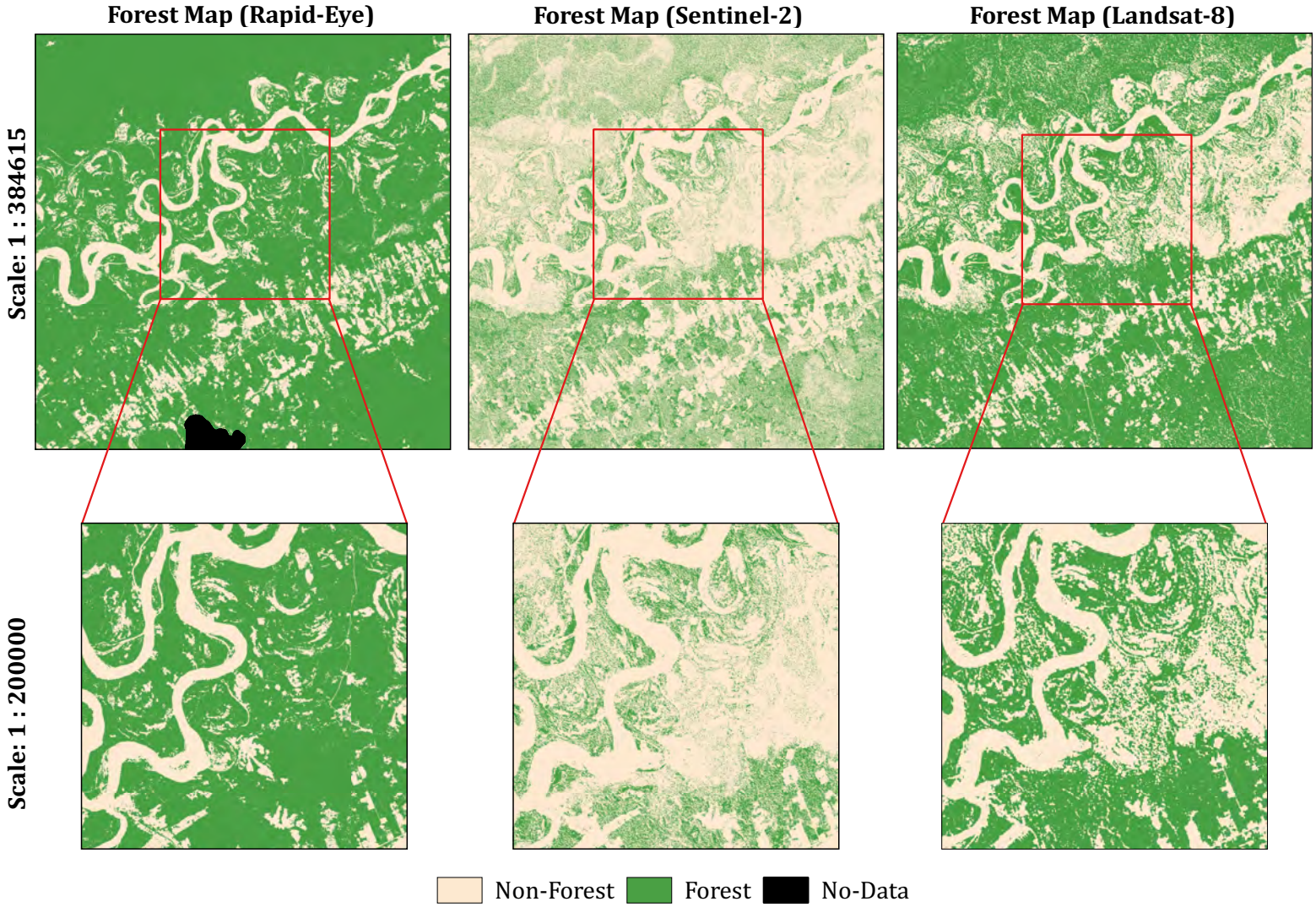

Figure 7: Final forest cover maps derived from high- and medium-resolution satellite imagery for Peru

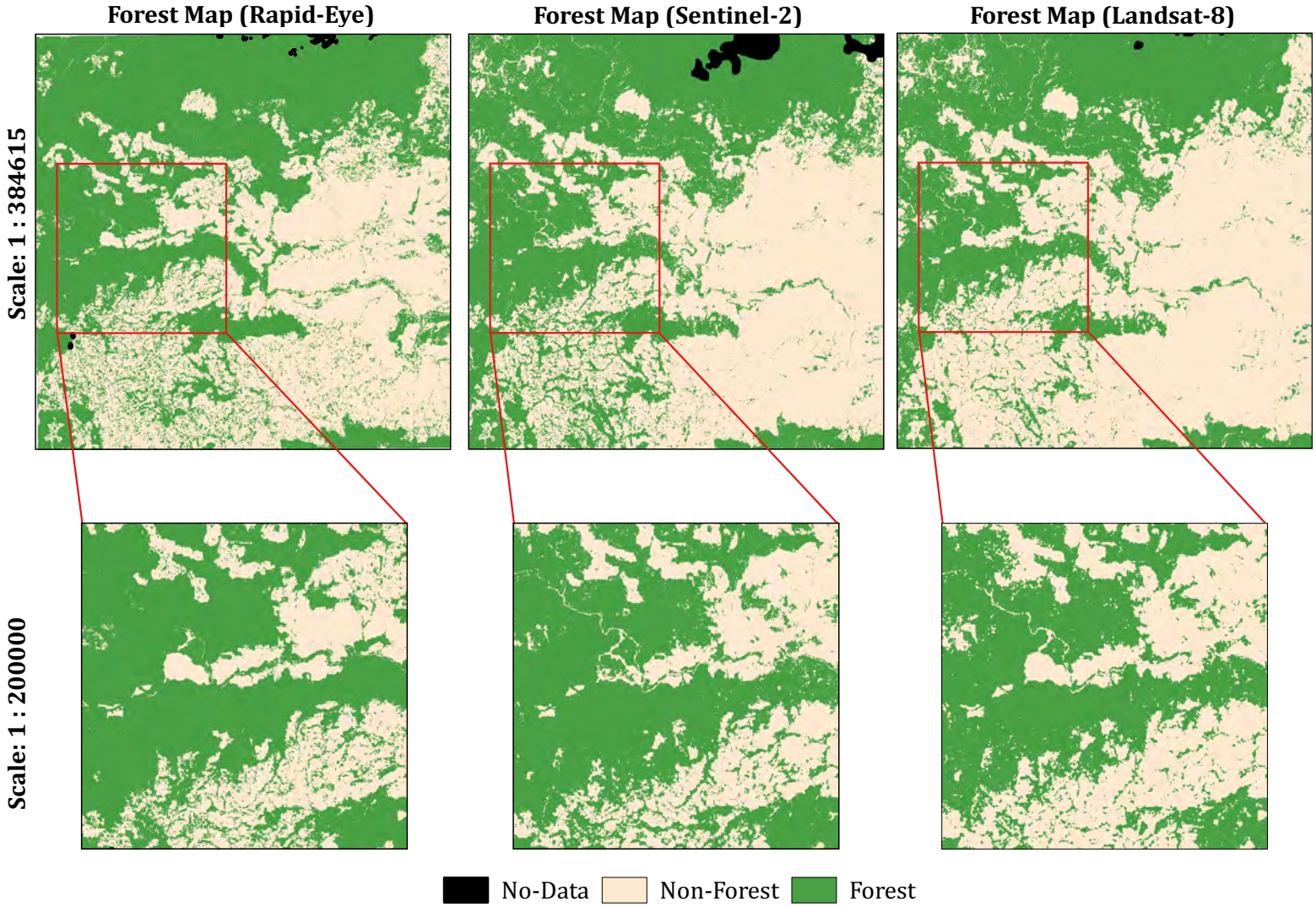

Figure 8: Final forest cover maps derived from high- and medium-resolution satellite imagery for Ethiopia

Corrections for bias are presented in Table 13 for Peru and Table 14 for Ethiopia. Low accuracy of Sentinel-2 and Landsat-8 based forest cover map for Peru results in considerable area adjustments. Area proportions for Sentinel-2 based forest map were corrected for 49.51% and 16.07% for Landsat based forest maps. Due to higher accuracy of RapidEye based forest map the area proportions update was 3.63%. Area proportion adjustments for the test site in Ethiopia were significantly smaller for all three satellite sensors in comparison to Peru test site. The main reason for low, 1.32% for RapidEye, 1.67% for Sentinel-2 and 11.92% for Landsat-8 based forest cover maps area updates, were the relatively high accuracies of the maps generated.

Satellite sensor	Mapped area		Corrected area	
	Forest	Non-forest	Forest	Non-forest
RapidEye	80.1%	19.9%	76.47% ± 2.30%	23.53% ± 2.30%
Sentinel-2	27.3%	72.7%	76.81% ± 5.77%	23.19% ± 5.77%
Landsat-8	61.8%	38.2%	77.87% ± 5.11%	22.13% ± 5.11%

Table 13: Mapped and corrected area proportions with confidence intervals for Peru

Satellite sensor	Mapped area		Corrected area	
	Forest	Non-forest	Forest	Non-forest
RapidEye	52.6%	47.4%	51.28% ± 2.60%	48.72% ± 2.60%
Sentinel-2	48.2%	51.8%	49.87% ± 4.08%	50.13% ± 4.08%
Landsat-8	41.8%	58.2%	53.72% ± 3.88%	46.28% ± 3.88%

Table 14: Mapped and corrected area proportions with confidence intervals for Ethiopia

5.2 Tree cover map accuracy test

The tree cover map is a result of CART classification which assigns each RapidEye image pixel to either tree or non-tree class. Tree cover maps for test sites in Peru and Ethiopia were assessed for accuracy in order to quantify the quality of generated tree cover maps. Output tree cover maps for Peru and Ethiopia test sites generated based on original

RapidEye imagery are shown in Figure 9. In the following step, forest cover maps were derived based on produced tree cover maps. Therefore, the accuracy of tree cover maps influences the accuracy of the forest cover maps generated from it. The main output of tree cover accuracy were the error matrices presented in Table 27 in Appendix for Peru and Table 28 in Appendix for Ethiopia. The error matrices are reported in terms of estimated area proportions $\hat{p}_{ij}$.

The proportion of map area classified correctly for the Ethiopia and Peru tree cover map is shown in the Table 15. The overall accuracies for both test sites were 91.98% ± 2.97% for Peru and 95.99% ± 2.20% for Ethiopia.

Test area	Overall accuracy
Peru	91.98% ± 2.97%
Ethiopia	95.99% ± 2.20%

Table 15: Tree cover map overall accuracies with confidence intervals

For Peru test site producer's and user's accuracies were relatively high showing that most pixels were classified correctly. The only exception was the user's accuracy of the non-tree class for Peru which was 82.61 % ± 4.26 %. This shows that the non-tree class area on the map was slightly overestimated. By comparing original and tree cover image it is evident that some forest areas were confused with the non-forest class. The tree cover map for Ethiopia had very high producer's and user's accuracies of tree and non-tree categories. Thus, according to the error matrix, all mapped classes are in considerable agreement with the reference data. Accuracy parameters with their 95% confidence intervals are shown in Table 16.

Test area	Producer's accuracy Tree	Producer's accuracy Non-tree	User's accuracy Tree	User's accuracy Non-tree
Peru	92.42% ± 3.08%	90.85% ± 5.74%	96.23% ± 2.14%	82.61% ± 4.26%
Ethiopia	94.25% ± 3.57%	97.60% ± 2.33%	97.32% ± 1.82%	94.84% ± 2.49%

Table 16: Tree cover map accuracy parameters with confidence intervals

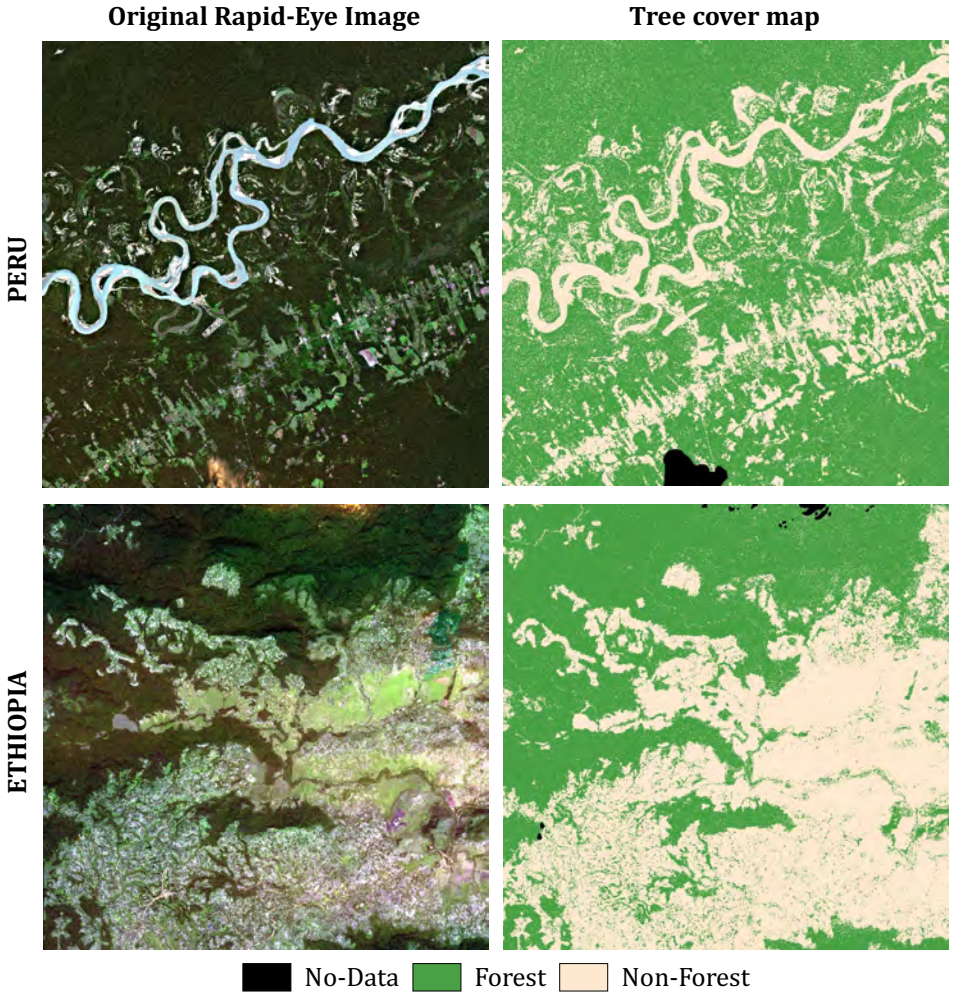

Figure 9: Original RapidEye images and derived tree cover maps for Peru and Ethiopia.

Results of the tree cover map accuracy test confirm high accuracy of tree cover maps derived from high-resolution satellite imagery. With accurate tree cover maps, high

accuracy of the input data for generating forest cover maps in the next processing step is provided and it thus contributes to the high accuracy of the final forest cover maps.

5.3 Minimum mapping unit forest map accuracy test

The MMU used in forest cover mapping is usually defined by the national forest definition and represents the unit at which the forest cover is mapped. Therefore, the MMU defines the level of mapped detail, which might affect the accuracy of forest cover mapping. Forest cover maps generated based on different MMUs were compared in Figure 10 for Peru and Figure 11 for Ethiopia. Considerable differences in generated forest cover maps were visually more pronounced for Peru than Ethiopia test site. Figure 10 of the test area in Peru shows obvious loss of highly fragmented non-forest patches which were mapped as forest on the maps that were generated based on bigger MMUs. Table 17 shows the increase of mapped forest cover proportion by increasing the size of MMU. Inversely, the non-forest proportion decreases by increasing the MMU. In the case of Peru, forest proportion difference between the smallest 15 by 15m MMU and the biggest 300 by 300m MMU is 14.40% or approximately 90000 ha. As can be seen from Figure 11 on forest cover maps generated for the test site in Ethiopia the general forest/non-forest pattern is preserved despite the generalisation of forest patches. Table 18 shows slightly increasing forest cover proportion if the MMU is increased. However, the absolute forest proportion difference is 5.23% or approximately 32700 ha for Ethiopia, which is nearly 3 times less than for the Peru test site.

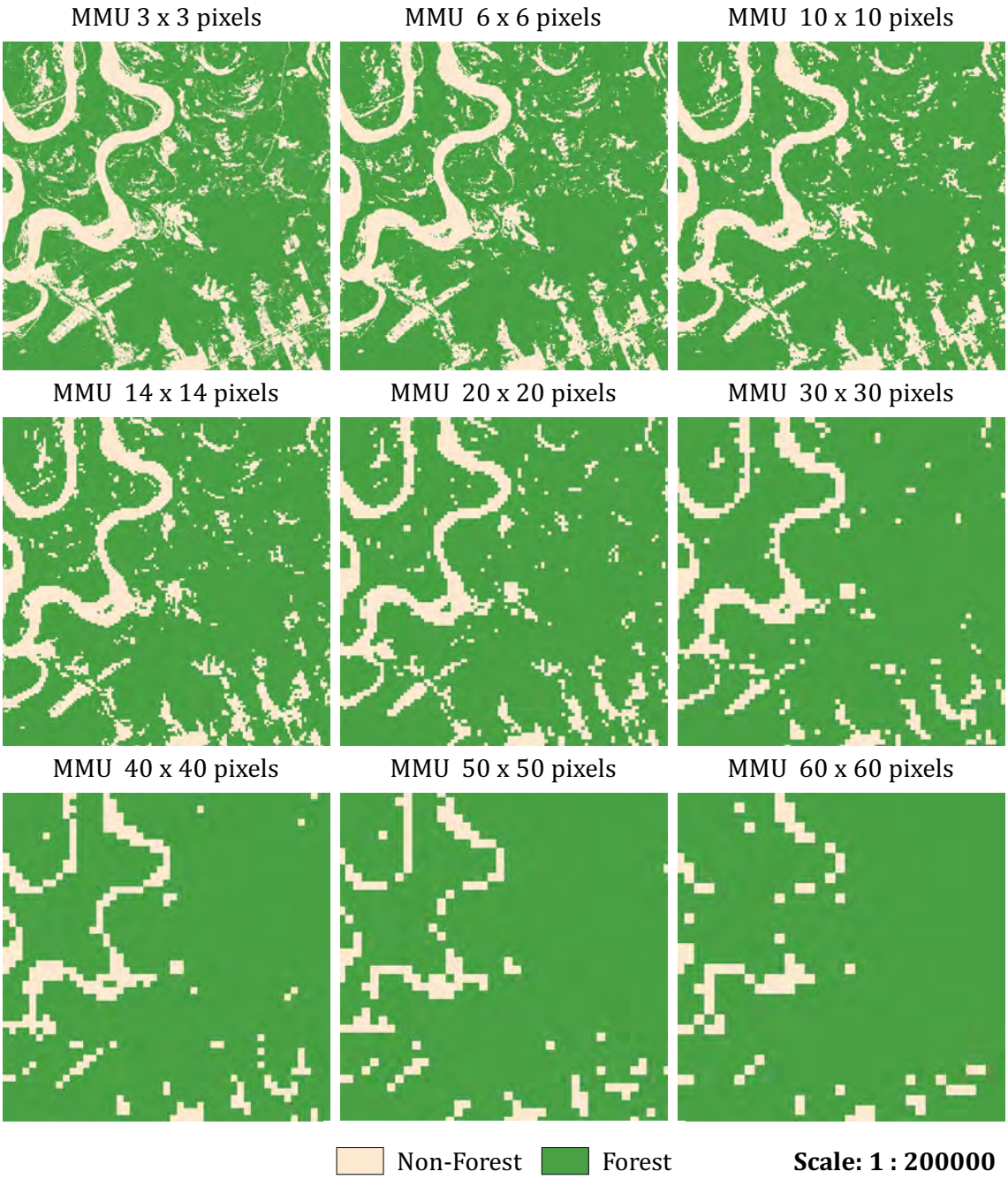

Figure 10: Zoomed in forest cover maps generated based on different MMUs for Peru

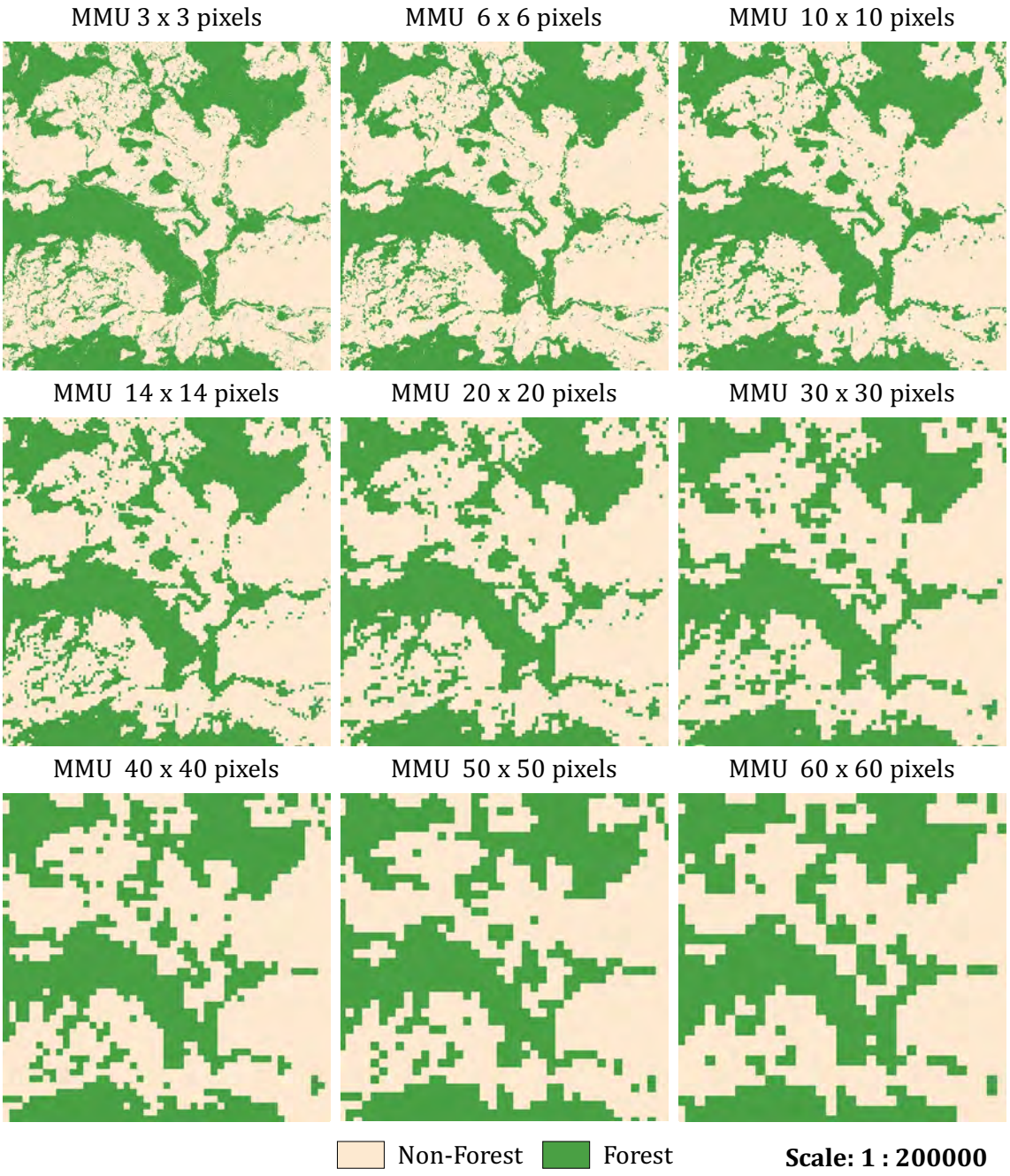

Figure 11: Zoomed in forest cover maps generated based on different MMUs for Ethiopia

MMU [m]	Forest proportion	Non-forest proportion
15 x 15	0.7950	0.2050
30 x 30	0.8125	0.1875
50 x 50	0.8312	0.1688
70 x 70	0.8486	0.1514
100 x 100	0.8670	0.1330
150 x 150	0.8923	0.1077
200 x 200	0.9105	0.0895
250 x 250	0.9237	0.0763
300 x 300	0.9391	0.0609

Table 17: Forest cover area map proportions for Peru

MMU [m]	Forest proportion	Non-forest proportion
15 x 15	0.5255	0.4745
30 x 30	0.5289	0.4711
50 x 50	0.5373	0.4627
70 x 70	0.5447	0.4553
100 x 100	0.5496	0.4504
150 x 150	0.5591	0.4409
200 x 200	0.5649	0.4351
250 x 250	0.5730	0.4270
300 x 300	0.5778	0.4222

Table 18: Forest cover area map proportions for Ethiopia

As described in the previous chapter, the MMU forest cover map accuracy test measures the accuracy of forest cover maps generated based on different MMUs. Accuracy parameters with their corresponding 95% confidence intervals for 5 accuracy assessment iterations are presented in Table 29 for Peru and in Table 30 for Ethiopia test sites in the Appendix. The resulting accuracy parameters for all 5 iterations were then averaged and presented in Table 19 for Peru and in Table 20 for Ethiopia.

As can be seen in Figure 12 the average overall map accuracy decreases with increasing MMU for both test sites. Overall accuracies in general remain quite high especially in

the case of Ethiopia. However, the overall accuracy difference between the minimum and maximum MMU grid size is higher, 14.21% for Peru than, 9.84% for Ethiopia forest cover maps. Similarly to the overall accuracy, producer's and user's accuracy parameters decrease by increasing the MMU. For Peru test site producer's forest and user's non-forest categories have high accuracy because a high proportion of map area was classified as forest and very low misclassification of non-forest samples occurred. These accuracies are stable and do not change significantly with respect to increasing MMU. In contrast, producer's accuracy of the non-forest class is very low and decreases drastically from 63.46% ±3.26% for 15 by 15m MMU to 18.83% ± 1.45% for 300 by 300 m MMU. Low non-forest producer's accuracy shows an under estimation of non-forest class on the map. Therefore, not enough of the map area is labelled as non-forest. Slightly lower user's accuracy of forest category, shows over-estimation of forest class on the map which increases by increasing MMU. Similarly stable, without significant change with respect to the MMU are producer's forest and user's non-forest classes for Ethiopia test site. As observed in the case of Peru, there is an evident drop in producer's non-forest and user's forest category accuracies for Ethiopia test site when the MMU is increased. However, the differences are smaller for Ethiopia than for Peru test area.

When interpreting the varying magnitude of accuracy parameters comparing Peru and Ethiopia test sites one should consider three significant differences between the two. First, the crown cover thresholds used for mapping forest cover differ. The 10% threshold was used for Peru and 20% for Ethiopia test site. Second, the proportion of trees/non-trees is around 50%/50% on Ethiopia and 70%/30% respectivelly on the Peru tree cover map. Third, the land cover is more fragmented on Peru than on Ethiopia tree cover map. These three parameters could account for test site-dependent differences in accuracy.

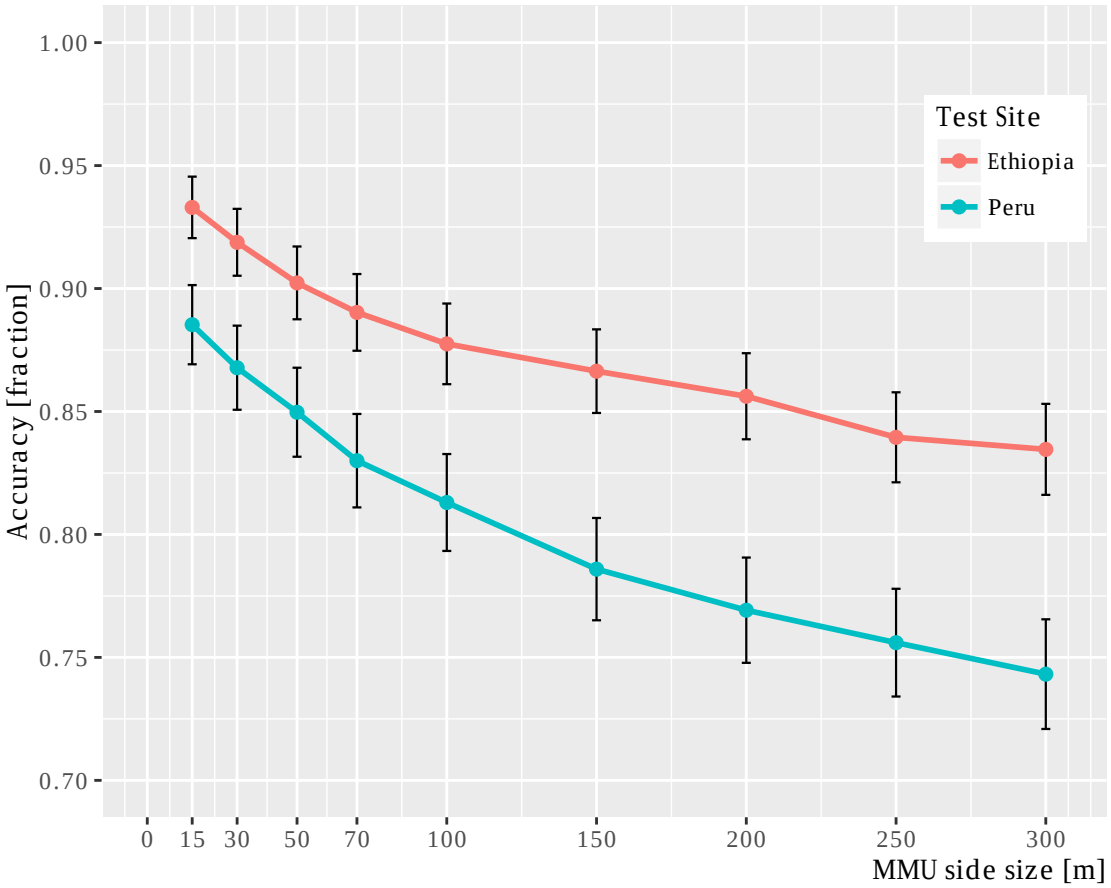

Figure 12: Average forest cover maps overall accuracies with corresponding confidence intervals with respect to MMU for Peru and Ethiopia.

This Master's thesis results show that overall accuracy of forest cover mapping decreases with increasing MMU for both test sites. The constant decrease is observed also for producer's non-forest and user's forest map category. The analysis of accuracy parameters and forest/non-forest class proportions on the map show that increasing MMU has the effect on the forest cover estimates. The MMU forest cover map accuracy test shows increasing MMU increases the forest cover estimations and therefore, decreases the accuracy of generated forest cover maps.

MMU [m]	Overall accuracy	Producer's Forest	Producer's Non-forest	User's Forest	User's Non-forest
15 x 15	0.8853 ± 0.0161	1.0000 ± 0.0000	0.6346 ± 0.0326	0.8568 ± 0.0180	1.0000 ± 0.0000
30 x 30	0.8678 ± 0.0171	0.9981 ± 0.0020	0.5867 ± 0.0317	0.8390 ± 0.0189	0.9932 ± 0.0031
50 x 50	0.8497 ± 0.0181	0.9981 ± 0.0024	0.5297 ± 0.0302	0.8208 ± 0.0197	0.9922 ± 0.0039
70 x 70	0.8300 ± 0.0190	0.9968 ± 0.0030	0.4701 ± 0.0283	0.8024 ± 0.0205	0.9854 ± 0.0054
100 x 100	0.8130 ± 0.0197	0.9978 ± 0.0028	0.4149 ± 0.0260	0.7860 ± 0.0211	0.9889 ± 0.0053
150 x 150	0.7859 ± 0.0208	0.9960 ± 0.0039	0.3325 ± 0.0224	0.7631 ± 0.0219	0.9744 ± 0.0081
200 x 200	0.7692 ± 0.0214	0.9975 ± 0.0030	0.2783 ± 0.0193	0.7483 ± 0.0223	0.9809 ± 0.0068
250 x 250	0.7560 ± 0.0219	0.9966 ± 0.0034	0.2337 ± 0.0172	0.7385 ± 0.0226	0.9695 ± 0.0086
300 x 300	0.7432 ± 0.0223	0.9972 ± 0.0031	0.1883 ± 0.0145	0.7286 ± 0.0229	0.9686 ± 0.0087

Table 19: Average forest cover maps accuracy parameters with confidence intervals for Peru

MMU [m]	Overall accuracy	Producer's Forest	Producer's Non-forest	User's Forest	User's Non-forest
15 x 15	0.9330 ± 0.0125	0.9944 ± 0.0000	0.8798 ± 0.0200	0.8775 ± 0.0168	0.9946 ± 0.0036
30 x 30	0.9188 ± 0.0136	0.9843 ± 0.0000	0.8623 ± 0.0208	0.8605 ± 0.0178	0.9845 ± 0.0062
50 x 50	0.9023 ± 0.0148	0.9752 ± 0.0028	0.8396 ± 0.0216	0.8398 ± 0.0188	0.9751 ± 0.0079
70 x 70	0.8903 ± 0.0156	0.9708 ± 0.0000	0.8211 ± 0.0221	0.8234 ± 0.0196	0.9704 ± 0.0087
100 x 100	0.8775 ± 0.0164	0.9602 ± 0.0021	0.8060 ± 0.0225	0.8109 ± 0.0201	0.9589 ± 0.0102
150 x 150	0.8664 ± 0.0170	0.9573 ± 0.0037	0.7878 ± 0.0229	0.7966 ± 0.0206	0.9549 ± 0.0106
200 x 200	0.8562 ± 0.0175	0.9536 ± 0.0022	0.7722 ± 0.0230	0.7836 ± 0.0211	0.9505 ± 0.0111
250 x 250	0.8395 ± 0.0183	0.9482 ± 0.0041	0.7471 ± 0.0232	0.7616 ± 0.0219	0.9440 ± 0.0118
300 x 300	0.8346 ± 0.0185	0.9432 ± 0.0042	0.7404 ± 0.0234	0.7595 ± 0.0219	0.9374 ± 0.0124

Table 20: Average forest cover maps accuracy parameters with confidence intervals for Ethiopia

6 CONCLUSION AND FUTURE WORK

The Image resolution forest map accuracy test quantified the accuracy of forest cover maps generated from different resolution satellite imagery. The analysis conducted on two test sites showed a general decrease in overall accuracy for forest cover maps derived from medium-resolution satellite imagery. Stable and high overall accuracy confirmed suitability of forest cover mapping methodology for high-resolution satellite imagery. In contrast, medium-resolution forest mapping methodology produced maps with unstable and low accuracy indicating that sub-pixel classification was not able to extract mixed pixels endmember fractions good enough to map forest cover accurately. Therefore, mixed tree/non-tree pixels present in medium-resolution satellite imagery could have an impact on the accuracy of forest cover maps. Results presented in chapter 5.1 show the accuracy of forest cover maps generated from high-resolution satellite imagery is higher than of those processed from medium-resolution satellite imagery. Thus, accuracy assessment confirmed the decrease of forest cover mapping accuracy when comparing high- and medium-resolution satellite data. The accuracy of medium-resolution based forest cover maps varied depending on the test site analyzed. The accuracy of Landsat-8 based forest cover map for Peru was higher than the accuracy of Sentinel-2 based forest cover map. Therefore, the anticipated outcome that the overall accuracy of forest cover maps decreases with decreasing resolution of satellite imagery used to map forest cannot be confirmed.

The Minimum mapping unit forest cover map accuracy test showed that the overall accuracy of forest cover maps decreases by increasing MMU to map forest for about 10% to 15% depending on the area tested. This matches the hypothesis anticipating decreasing overall accuracy of forest cover maps with increasing the size of MMU for mapping forest cover. In addition, the increase of forest class proportion on the map was observed for increasing MMU for both test sites.

Highly accurate forest cover maps are essential to detect and measure changes in forest cover for countries participating in REDD+. This thesis provides an accuracy measurement of what are the consequences of mapping forest cover from high- and medium-resolution satellite imagery. Highly accurate forest cover maps can be generated from high-resolution satellite imagery. Moreover, the method used to map forest from medium-resolution imagery did not provide accurate sub-pixel classification results. Since the accuracy loss when working with medium-resolution satellite imagery is evident, the effort using high-resolution imagery compensates for high forest cover map accuracy.

The medium-resolution forest mapping method could be improved by using ground visits data to define pure pixel endmembers. Hence, derived endmember fraction images might be more accurate. Similarly, if available, ground data used as a source of reference data in accuracy assessment could improve the overall accuracy assessment. Another obvious limitation of sub-pixel classification method is varying forest map accuracy for different test sites. This indicates that the forest map accuracy is whether landscape or crown cover threshold dependent when applying sub-pixel classification methodology. Therefore, further research would need to be conducted to test the effects of landscape properties and crown cover threshold on the accuracy of medium-resolution based forest mapping.

The size of the MMU chosen affects the accuracy of generated forest cover map. Therefore, the MMU needs to be selected carefully considering the loss of accuracy if the MMU used is too large. Generally, smaller MMUs contribute to higher forest cover map accuracy and are preferred to be applied in forest cover mapping. Since the accuracy results and land cover proportion differences varied depending on the test site analysed, areas with diverse land cover proportions should be tested in further research.

Accuracy analysis in this Master's thesis was conducted on two distinctive test sites. Of-

ficial national forest definitions were applied to the real world examples for which forest cover maps were derived. Therefore, the outcomes of this research can serve countries participating in REDD+ programme to decide which satellite imagery spatial resolution and MMU to use for forest cover mapping, deforestation and forest degradation monitoring.

References

[1] UN-REDD, 2016. http://www.unredd.net. (Accessed November 15, 2016).

[2] GOFC-GOLD, 2015. IA sourcebook of methods and procedures for monitoring and reporting anthropogenic greenhouse gas emissions and removals associated with deforestation, gains and losses of carbon stocks in forests remaining forests, and forestation. GOFC-GOLD Report version COP21-1.
Available at: http://www.gfoi.org/wp-content/uploads/2015/03/MGD_copyedited06082014.pdf. (Accessed November 17, 2016).

[3] Bernard, F., Minang, P. A., 2011. Strengthening Measurement, Reporting and Verification (MRV) for REDD+. International Institute for Sustainable development.
Available at: https://www.iisd.org/sites/default/files/publications/redd_strengthening_mrv_kenya.pdf. (Accessed November 16, 2016).

[4] UNFCCC, 2002. Report of the Conference of the Parties on its seventh session, held at Marrakesh from 29 October to 10 November 2001. UNFCCC.
Available at: http://unfccc.int/resource/docs/cop7/13a01.pdf. (Accessed November 18, 2016).

[5] ForMoSa, 2016.
http://www.formosa.global/. (Accessed November 21, 2016).

[6] Magdon, P., Fischer C., Fuchs H., Kleinn, C., 2014. Translating criteria of international forest definitions into remote sensing image analysis. Remote Sensing of Environment, 149, pp. 252-262.

[7] Asner G. P., Knapp D. E., Balaji A., Páez-Acosta, G., 2009. Automated mapping of tropical deforestation and forest degradation: CLASlite. Journal of Applied Remote Sensing, 3(1).

[8] Kleinn, C., 2001. A cautionary note on the minimum crown cover criterion in forest definitions. Canadian Journal of Forest Research, 31(2), pp. 350-356.

[9] Magdon, P., Kleinn, C., 2012. Uncertainties of forest area estimates caused by the minimum crown cover criterion: A scale issue relevant to forest cover monitoring. Environmental Monitoring and Assessment, 185(6), pp. 5345-5360.

[10] Stehman, S. V., Czaplewski R. L., 1998. Design and analysis for thematic map accuracy assessment: Fundamental principles. Remote Sensing of the Environment, 64, pp. 331-344.

[11] Congalton, R. G., Green, K., 2009. Assessing the accuracy of remotely sensed data: Principles and practices. Boca Raton: CRC Press, 2nd edition.

[12] Olofsson, P., Foody, G. M., Herold, M., Stehman, S. V., Woodcock, C. E., Wulder, M. A., 2014. Good practices for estimating area and assessing accuracy of land change. Remote Sensing of Environment, 148, pp. 42-57.

[13] Food and Agriculture Organisation of the United Nations, 2016. Map accuracy assessment and area estimation: A practical guide. [pdf] Rome: Food and Agriculture Organisation of the United Nations.
Available at:`http://www.fao.org/3/a-i5601e.pdf`. (Accessed July 1, 2016).

[14] Foody, G. M., 2008. Sample size determination for image classification accuracy assessment and comparison. Proceedings of the 8th International Symposium on Spatial accuracy assessment in natural resources and environmental sciences. Shanghai, P.R. China, June 25-27, pp. 154-162.

[15] McRoberts, R. E., Walters B.F., 2012. Statistical inference for remote sensing-based estimates of net deforestation. Remote Sensing of the Environment, 124, pp. 394-401.

[16] Spot (Take5), 2017.
https://www.spot-take5.org/client/#/home. (Accessed March 17, 2017).

[17] REDD Project in Brazil Nut Concessions in Madre de Dios, 2014.
Available at: https://s3.amazonaws.com/CCBA/Projects/REDD_Project_in_Brazil_Nut_Concession_in_Madre_de_Dios/Validation/Casta%C3%B1eros+REDD+Project+CCB+PD+v6.pdf. (Accessed December 19, 2016).

[18] Bekele M, Tesfaye Y, Mohammed Z, Zewdie S, Tebikew Y, Brockhaus M and Kassa H., 2015. The context of REDD+ in Ethiopia: Drivers, agents and institutions. Occasional Paper 127. Bogor, Indonesia: CIFOR.
Available at: http://www.cifor.org/publications/pdf_files/OccPapers/OP-127.pdf. (Accessed December 19, 2016)

[19] Ethiopia's forest reference level submission to the UNFCCC, 2016.
Available at: http://redd.unfccc.int/files/2016_submission_frel_ethiopia.pdf. (Accesses December 11, 2016).

[20] Peru's submission of a Forest Reference Emission Level (FREL) for reducing emissions from deforestation in the Peruvian Amazon, 2015.
Available at: http://redd.unfccc.int/files/2015_submission_frel_peru_en.pdf. (Accessed December 11, 2016).

[21] Chuvieco, E., 2016. Fundamentals of Satellite Remote Sensing: An Environmental Approach. Boca Raton: CRC Press, 2nd edition.

[22] Black Bridge. Technical Specifications ForMoSa project. [Technical report].

[23] Breiman, L., Friedman, J.H., Olshen, R.A., Stone, C.J., 1984. Classification and Regression Trees. Boca Raton: Chapman and Hall.

[24] PCI Geomatics, 2016.
http://www.pcigeomatics.com/geomatica-help/references/hyperspec_r/advhyperspec4n126.html.

[25] PCI Geomatics, 2016.
http://www.pcigeomatics.com/geomatica-help/references/pcifunction_r/python/p_csg2.html.

[26] PCI Geomatics, 2016.
http://www.pcigeomatics.com/geomatica-help/references/pcifunction_r/modeler/m_unmix.html.

[27] Köhl, M., Magnussen, S., Marchetti, M., 2006. Sampling Methods, Remote Sensing and GIS Multiresource Forest Inventory. Berlin; Heidelberg: Springer.

APPENDICES

APPENDIX A: Error matices of Image resolution forest map accuracy test

APPENDIX B: Error matices of Tree cover map accuracy test

APPENDIX C: Accuracy parameters of MMU forest cover map test iterations

APPENDIX D: Overally accuracy graphs of MMU forest cover map test iterations

APPENDIX A: Error matices of Image resolution forest map accuracy test

		Reference			
		Forest	Non-forest	Map marginal proportions	User's accuracy
Map	Forest	0.7594	0.0416	0.801	0.9481
	Non-forest	0.0028	0.1962	0.199	0.9861
	True marginal proportions	0.7622	0.2378	1	
	Producer's accuracy	0.9964	0.8251		0.9556

Table 21: Forest cover map error matrix for Peru Rapid-Eye

		Reference			
		Forest	Non-forest	Map marginal proportions	User's accuracy
Map	Forest	0.2647	0.0083	0.273	0.9697
	Non-forest	0.4654	0.2616	0.727	0.3598
	True marginal proportions	0.7301	0.2699	1	
	Producer's accuracy	0.3626	0.9693		0.5263

Table 22: Forest cover map error matrix for Peru Sentinel-2

		Reference			
		Forest	Non-forest	Map marginal proportions	User's accuracy
Map	Forest	0.5796	0.0384	0.618	0.9379
	Non-forest	0.1791	0.2029	0.382	0.5313
	True marginal proportions	0.7587	0.2413	1	
	Producer's accuracy	0.7640	0.8409		0.7825

Table 23: Forest cover map error matrix for Peru Landsat

		Reference			
		Forest	Non-forest	Map marginal proportions	User's accuracy
Map	Forest	0.4255	0.0565	0.482	0.8828
	Non-forest	0.0735	0.4445	0.518	0.8581
	True marginal proportions	0.4990	0.5010	1	
	Producer's accuracy	0.8527	0.8872		0.8700

Table 24: Forest cover map error matrix for Ethiopia Sentinel-2

		Reference			
		Forest	Non-forest	Map marginal proportions	User's accuracy
Map	Forest	0.4933	0.0327	0.526	0.9379
	Non-forest	0.0202	0.4538	0.474	0.9574
	True marginal proportions	0.5135	0.4865	1	
	Producer's accuracy	0.9607	0.9328		0.9472

Table 25: Forest cover map error matrix for Ethiopia Rapid-Eye

		Reference			
		Forest	Non-forest	Map marginal proportions	User's accuracy
Map	Forest	0.4114	0.0066	0.418	0.9841
	Non-forest	0.1257	0.4563	0.582	0.7841
	True marginal proportions	0.5370	0.4630	1	
	Producer's accuracy	0.7660	0.9857		0.8677

Table 26: Forest cover map error matrix for Ethiopia Landsat

APPENDIX B: Error matices of Tree cover map accuracy test

		Reference			
		Tree	Non-tree	Map marginal proportions	User's accuracy
Map	Tree	0.6620	0.0260	0.688	0.9623
	Non-tree	0.0543	0.2577	0.312	0.8261
	True marginal proportions	0.7163	0.2837	1	
	Producer's accuracy	0.9242	0.9085		0.9198

Table 27: Tree cover map error matrix for Peru

		Reference			
		Tree	Non-tree	Map marginal proportions	User's accuracy
Map	Tree	0.4525	0.0125	0.465	0.9732
	Non-tree	0.0276	0.5074	0.535	0.9484
	True marginal proportions	0.4801	0.5199	1	
	Producer's accuracy	0.9425	0.9760		0.9599

Table 28: Tree cover map error matrix for Ethiopia

APPENDIX C: Accuracy parameters of MMU forest cover map test iterations

Interation	MMU [m]	Overall accuracy	Producer's accuracy Forest	Producer's accuracy Non-forest	User's accuracy Forest	User's accuracy Non-forest
1	15 x 15	0.8791 ± 0.0165	1.0000 ± 0.0000	0.6221 ± 0.0320	0.8491 ± 0.0184	1.0000 ± 0.0000
	30 x 30	0.8601 ± 0.0176	0.9959 ± 0.0040	0.5733 ± 0.0312	0.8314 ± 0.0193	0.9850 ± 0.0062
	50 x 50	0.8442 ± 0.0183	0.9989 ± 0.0020	0.5203 ± 0.0295	0.8133 ± 0.0200	0.9958 ± 0.0033
	70 x 70	0.8249 ± 0.0192	0.9959 ± 0.0039	0.4625 ± 0.0279	0.7971 ± 0.0207	0.9815 ± 0.0069
	100 x 100	0.8071 ± 0.0200	0.9979 ± 0.0029	0.4073 ± 0.0253	0.7792 ± 0.0213	0.9892 ± 0.0053
	150 x 150	0.7842 ± 0.0209	0.9969 ± 0.0034	0.3313 ± 0.0220	0.7604 ± 0.0219	0.9806 ± 0.0071
	200 x 200	0.7621 ± 0.0216	0.9967 ± 0.0035	0.2713 ± 0.0188	0.7410 ± 0.0225	0.9752 ± 0.0080
	250 x 250	0.7508 ± 0.0220	0.9978 ± 0.0029	0.2312 ± 0.0164	0.7319 ± 0.0228	0.9806 ± 0.0071
	300 x 300	0.7424 ± 0.0223	0.9981 ± 0.0027	0.1889 ± 0.0141	0.7270 ± 0.0229	0.9787 ± 0.0074
2	15 x 15	0.8916 ± 0.0157	1.0000 ± 0.0000	0.6474 ± 0.0332	0.8647 ± 0.0176	1.0000 ± 0.0000
	30 x 30	0.8680 ± 0.0171	1.0000 ± 0.0000	0.5861 ± 0.0314	0.8376 ± 0.0190	1.0000 ± 0.0000
	50 x 50	0.8497 ± 0.0181	0.9977 ± 0.0029	0.5296 ± 0.0303	0.8211 ± 0.0197	0.9908 ± 0.0049
	70 x 70	0.8382 ± 0.0187	0.9978 ± 0.0029	0.4826 ± 0.0291	0.8112 ± 0.0201	0.9901 ± 0.0051
	100 x 100	0.8177 ± 0.0196	0.9977 ± 0.0029	0.4211 ± 0.0265	0.7916 ± 0.0209	0.9883 ± 0.0055
	150 x 150	0.7871 ± 0.0208	0.9940 ± 0.0047	0.3323 ± 0.0229	0.7659 ± 0.0218	0.9621 ± 0.0098
	200 x 200	0.7751 ± 0.0213	0.9954 ± 0.0041	0.2814 ± 0.0203	0.7564 ± 0.0221	0.9649 ± 0.0095
	250 x 250	0.7630 ± 0.0217	0.9955 ± 0.0041	0.2375 ± 0.0181	0.7469 ± 0.0224	0.9588 ± 0.0102
	300 x 300	0.7461 ± 0.0222	0.9962 ± 0.0037	0.1885 ± 0.0151	0.7325 ± 0.0228	0.9565 ± 0.0105

Interation	MMU [m]	Overall accuracy	Producer's accuracy Forest	Producer's accuracy Non-forest	User's accuracy Forest	User's accuracy Non-forest
3	15 x 15	0.8922 ± 0.0157	1.0000 ± 0.0000	0.6487 ± 0.0333	0.8655 ± 0.0176	1.0000 ± 0.0000
	30 x 30	0.8743 ± 0.0169	0.9959 ± 0.0039	0.5999 ± 0.0327	0.8489 ± 0.0185	0.9847 ± 0.0063
	50 x 50	0.8541 ± 0.0179	0.9958 ± 0.0040	0.5374 ± 0.0311	0.8280 ± 0.0194	0.9828 ± 0.0067
	70 x 70	0.8289 ± 0.0192	0.9933 ± 0.0050	0.4679 ± 0.0288	0.8038 ± 0.0205	0.9697 ± 0.0088
	100 x 100	0.8158 ± 0.0197	0.9977 ± 0.0029	0.4185 ± 0.0263	0.7894 ± 0.0210	0.9882 ± 0.0056
	150 x 150	0.7915 ± 0.0207	0.9955 ± 0.0041	0.3381 ± 0.0231	0.7697 ± 0.0217	0.9714 ± 0.0086
	200 x 200	0.7766 ± 0.0212	0.9977 ± 0.0029	0.2850 ± 0.0199	0.7562 ± 0.0221	0.9825 ± 0.0068
	250 x 250	0.7625 ± 0.0217	0.9956 ± 0.0040	0.2373 ± 0.0180	0.7463 ± 0.0224	0.9596 ± 0.0101
	300 x 300	0.7529 ± 0.0220	0.9979 ± 0.0028	0.1951 ± 0.0150	0.7385 ± 0.0226	0.9756 ± 0.0079
4	15 x 15	0.8814 ± 0.0164	1.0000 ± 0.0000	0.6265 ± 0.0323	0.8519 ± 0.0183	1.0000 ± 0.0000
	30 x 30	0.8662 ± 0.0172	1.0000 ± 0.0000	0.5829 ± 0.0313	0.8354 ± 0.0191	1.0000 ± 0.0000
	50 x 50	0.8501 ± 0.0181	0.9979 ± 0.0028	0.5303 ± 0.0303	0.8213 ± 0.0197	0.9917 ± 0.0047
	70 x 70	0.8279 ± 0.0191	1.0000 ± 0.0000	0.4673 ± 0.0276	0.7973 ± 0.0207	1.0000 ± 0.0000
	100 x 100	0.8108 ± 0.0198	0.9989 ± 0.0021	0.4124 ± 0.0256	0.7827 ± 0.0212	0.9944 ± 0.0038
	150 x 150	0.7785 ± 0.0211	0.9964 ± 0.0037	0.3252 ± 0.0216	0.7544 ± 0.0222	0.9776 ± 0.0076
	200 x 200	0.7617 ± 0.0216	0.9987 ± 0.0022	0.2729 ± 0.0183	0.7390 ± 0.0226	0.9904 ± 0.0050
	250 x 250	0.7507 ± 0.0221	0.9954 ± 0.0041	0.2284 ± 0.0171	0.7335 ± 0.0228	0.9592 ± 0.0102
	300 x 300	0.7339 ± 0.0226	0.9951 ± 0.0042	0.1800 ± 0.0146	0.7202 ± 0.0231	0.9452 ± 0.0117
5	15 x 15	0.8823 ± 0.0163	1.0000 ± 0.0000	0.6284 ± 0.0323	0.8531 ± 0.0182	1.0000 ± 0.0000
	30 x 30	0.8704 ± 0.0170	0.9990 ± 0.0020	0.5911 ± 0.0318	0.8415 ± 0.0188	0.9963 ± 0.0031
	50 x 50	0.8506 ± 0.0180	1.0000 ± 0.0000	0.5308 ± 0.0300	0.8202 ± 0.0197	1.0000 ± 0.0000
	70 x 70	0.8303 ± 0.0190	0.9969 ± 0.0034	0.4704 ± 0.0283	0.8026 ± 0.0205	0.9859 ± 0.0061
	100 x 100	0.8135 ± 0.0197	0.9969 ± 0.0034	0.4152 ± 0.0262	0.7874 ± 0.0210	0.9841 ± 0.0064
	150 x 150	0.7882 ± 0.0207	0.9969 ± 0.0034	0.3355 ± 0.0224	0.7650 ± 0.0218	0.9803 ± 0.0071
	200 x 200	0.7706 ± 0.0213	0.9989 ± 0.0020	0.2807 ± 0.0190	0.7487 ± 0.0223	0.9917 ± 0.0047
	250 x 250	0.7532 ± 0.0219	0.9988 ± 0.0021	0.2341 ± 0.0163	0.7338 ± 0.0227	0.9894 ± 0.0053
	300 x 300	0.7408 ± 0.0223	0.9988 ± 0.0021	0.1889 ± 0.0137	0.7248 ± 0.0230	0.9870 ± 0.0058

Table 29: Forest cover maps accuracy parameters with confidence intervals for Peru

Interation	MMU [m]	Overall accuracy	Producer's accuracy Forest	Producer's accuracy Non-forest	User's accuracy Forest	User's accuracy Non-forest
1	15 x 15	0.9250 ± 0.0131	0.9897 ± 0.0075	0.8698 ± 0.0204	0.8664 ± 0.0175	0.9900 ± 0.0051
	30 x 30	0.9046 ± 0.0147	0.9735 ± 0.0119	0.8461 ± 0.0213	0.8429 ± 0.0187	0.9741 ± 0.0082
	50 x 50	0.8996 ± 0.0151	0.9663 ± 0.0131	0.8407 ± 0.0218	0.8428 ± 0.0187	0.9658 ± 0.0093
	70 x 70	0.8831 ± 0.0160	0.9662 ± 0.0133	0.8126 ± 0.0223	0.8140 ± 0.0200	0.9659 ± 0.0093
	100 x 100	0.8675 ± 0.0169	0.9557 ± 0.0150	0.7929 ± 0.0226	0.7960 ± 0.0207	0.9549 ± 0.0107
	150 x 150	0.8659 ± 0.0169	0.9632 ± 0.0138	0.7835 ± 0.0228	0.7903 ± 0.0209	0.9617 ± 0.0098
	200 x 200	0.8457 ± 0.0180	0.9495 ± 0.0159	0.7584 ± 0.0230	0.7677 ± 0.0217	0.9470 ± 0.0115
	250 x 250	0.8364 ± 0.0184	0.9492 ± 0.0159	0.7419 ± 0.0231	0.7548 ± 0.0221	0.9458 ± 0.0116
	300 x 300	0.8222 ± 0.0190	0.9378 ± 0.0173	0.7249 ± 0.0232	0.7416 ± 0.0225	0.9326 ± 0.0129
2	15 x 15	0.9288 ± 0.0128	0.9940 ± 0.0058	0.8731 ± 0.0203	0.8698 ± 0.0173	0.9941 ± 0.0039
	30 x 30	0.9224 ± 0.0133	0.9895 ± 0.0076	0.8647 ± 0.0207	0.8626 ± 0.0177	0.9897 ± 0.0052
	50 x 50	0.9038 ± 0.0147	0.9776 ± 0.0109	0.8403 ± 0.0216	0.8405 ± 0.0188	0.9776 ± 0.0076
	70 x 70	0.9003 ± 0.0149	0.9807 ± 0.0102	0.8310 ± 0.0219	0.8335 ± 0.0191	0.9803 ± 0.0071
	100 x 100	0.8853 ± 0.0159	0.9663 ± 0.0131	0.8144 ± 0.0224	0.8200 ± 0.0197	0.9651 ± 0.0094
	150 x 150	0.8660 ± 0.0170	0.9584 ± 0.0145	0.7862 ± 0.0229	0.7949 ± 0.0207	0.9563 ± 0.0105
	200 x 200	0.8600 ± 0.0173	0.9560 ± 0.0148	0.7763 ± 0.0231	0.7886 ± 0.0210	0.9528 ± 0.0109
	250 x 250	0.8393 ± 0.0182	0.9495 ± 0.0158	0.7460 ± 0.0231	0.7600 ± 0.0219	0.9458 ± 0.0116
	300 x 300	0.8365 ± 0.0184	0.9466 ± 0.0161	0.7412 ± 0.0234	0.7600 ± 0.0219	0.9413 ± 0.0121
3	15 x 15	0.9457 ± 0.0113	0.9985 ± 0.0029	0.8983 ± 0.0192	0.8981 ± 0.0155	0.9985 ± 0.0020
	30 x 30	0.9273 ± 0.0130	0.9860 ± 0.0087	0.8751 ± 0.0204	0.8752 ± 0.0170	0.9860 ± 0.0060
	50 x 50	0.9161 ± 0.0139	0.9759 ± 0.0111	0.8616 ± 0.0212	0.8655 ± 0.0175	0.9751 ± 0.0080
	70 x 70	0.9005 ± 0.0150	0.9694 ± 0.0125	0.8383 ± 0.0220	0.8441 ± 0.0186	0.9681 ± 0.0090
	100 x 100	0.8922 ± 0.0156	0.9574 ± 0.0143	0.8312 ± 0.0225	0.8414 ± 0.0187	0.9543 ± 0.0107
	150 x 150	0.8754 ± 0.0167	0.9464 ± 0.0157	0.8081 ± 0.0232	0.8237 ± 0.0195	0.9409 ± 0.0121
	200 x 200	0.8762 ± 0.0166	0.9536 ± 0.0148	0.8030 ± 0.0233	0.8209 ± 0.0197	0.9481 ± 0.0114
	250 x 250	0.8468 ± 0.0181	0.9337 ± 0.0172	0.7653 ± 0.0239	0.7886 ± 0.0209	0.9249 ± 0.0135
	300 x 300	0.8473 ± 0.0181	0.9353 ± 0.0169	0.7632 ± 0.0240	0.7905 ± 0.0209	0.9251 ± 0.0135

Interation	MMU [m]	Overall accuracy	Producer's accuracy Forest	Producer's accuracy Non-forest	User's accuracy Forest	User's accuracy Non-forest
4	15 x 15	0.9394 ± 0.0119	0.9958 ± 0.0048	0.8896 ± 0.0197	0.8886 ± 0.0162	0.9958 ± 0.0033
	30 x 30	0.9252 ± 0.0132	0.9886 ± 0.0079	0.8698 ± 0.0206	0.8688 ± 0.0173	0.9887 ± 0.0054
	50 x 50	0.9022 ± 0.0147	0.9864 ± 0.0087	0.8326 ± 0.0216	0.8297 ± 0.0193	0.9867 ± 0.0059
	70 x 70	0.8825 ± 0.0161	0.9662 ± 0.0133	0.8116 ± 0.0223	0.8128 ± 0.0200	0.9660 ± 0.0093
	100 x 100	0.8741 ± 0.0166	0.9620 ± 0.0140	0.7995 ± 0.0225	0.8028 ± 0.0204	0.9612 ± 0.0099
	150 x 150	0.8773 ± 0.0164	0.9628 ± 0.0137	0.8011 ± 0.0229	0.8119 ± 0.0201	0.9603 ± 0.0100
	200 x 200	0.8571 ± 0.0174	0.9557 ± 0.0149	0.7721 ± 0.0231	0.7835 ± 0.0212	0.9528 ± 0.0109
	250 x 250	0.8413 ± 0.0181	0.9589 ± 0.0146	0.7445 ± 0.0229	0.7554 ± 0.0221	0.9566 ± 0.0105
	300 x 300	0.8510 ± 0.0177	0.9583 ± 0.0144	0.7566 ± 0.0234	0.7760 ± 0.0214	0.9537 ± 0.0108
5	15 x 15	0.9259 ± 0.0130	0.9941 ± 0.0058	0.8685 ± 0.0204	0.8643 ± 0.0176	0.9943 ± 0.0039
	30 x 30	0.9146 ± 0.0140	0.9838 ± 0.0094	0.8557 ± 0.0210	0.8528 ± 0.0182	0.9842 ± 0.0064
	50 x 50	0.8898 ± 0.0156	0.9700 ± 0.0126	0.8228 ± 0.0219	0.8205 ± 0.0197	0.9705 ± 0.0087
	70 x 70	0.8848 ± 0.0159	0.9716 ± 0.0123	0.8122 ± 0.0222	0.8124 ± 0.0200	0.9716 ± 0.0085
	100 x 100	0.8684 ± 0.0168	0.9596 ± 0.0144	0.7923 ± 0.0225	0.7942 ± 0.0208	0.9591 ± 0.0102
	150 x 150	0.8475 ± 0.0178	0.9559 ± 0.0152	0.7603 ± 0.0226	0.7624 ± 0.0219	0.9554 ± 0.0106
	200 x 200	0.8419 ± 0.0181	0.9535 ± 0.0155	0.7512 ± 0.0228	0.7572 ± 0.0220	0.9520 ± 0.0110
	250 x 250	0.8335 ± 0.0185	0.9497 ± 0.0159	0.7377 ± 0.0230	0.7491 ± 0.0223	0.9468 ± 0.0115
	300 x 300	0.8158 ± 0.0192	0.9381 ± 0.0174	0.7159 ± 0.0230	0.7294 ± 0.0228	0.9341 ± 0.0127

Table 30: Forest cover maps accuracy parameters with confidence intervals for Ethiopia

APPENDIX D: Overally accuracy graphs of MMU forest cover map test iterations

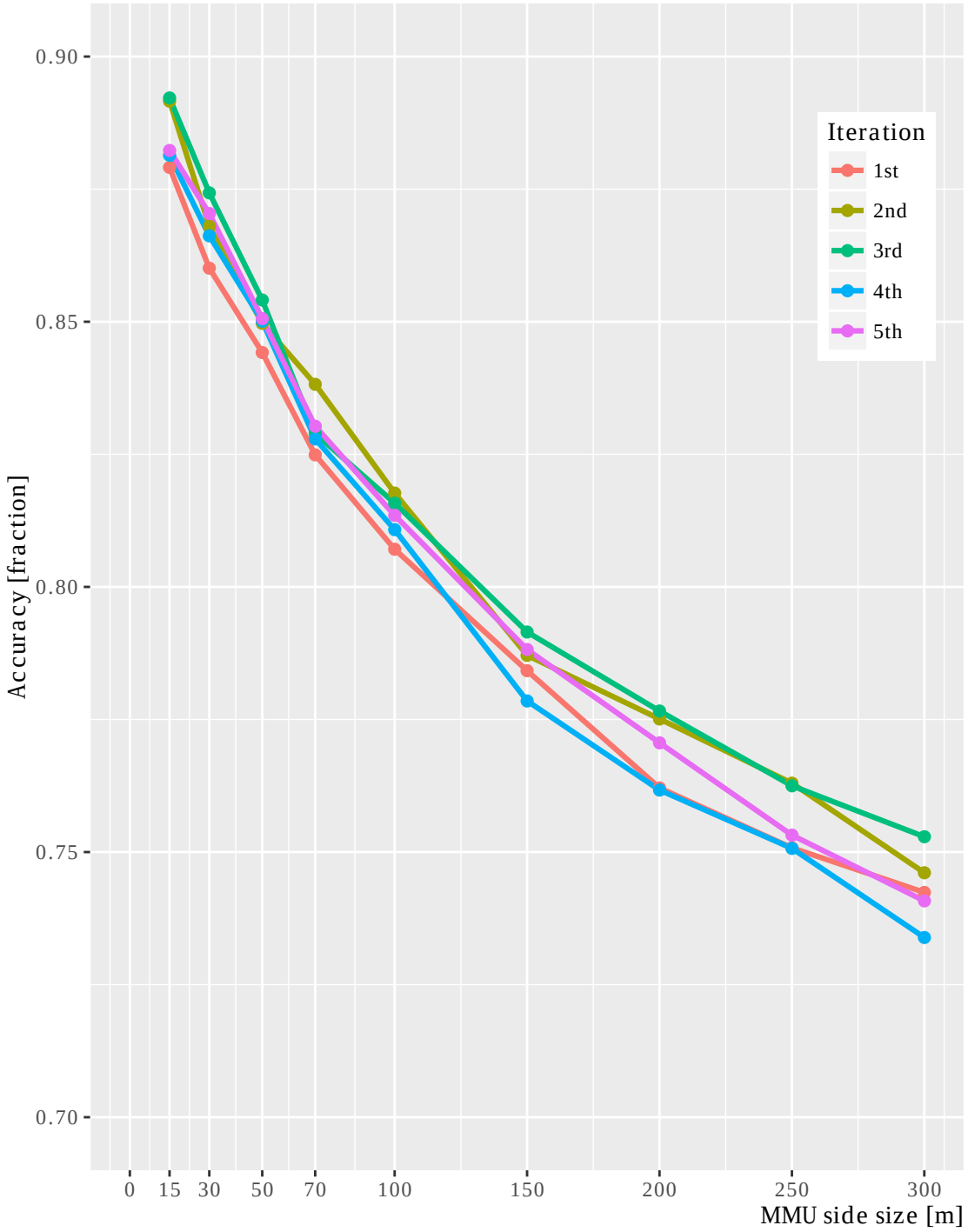

Figure 13: 5 iterations overall accuracies for all MMUs in Peru

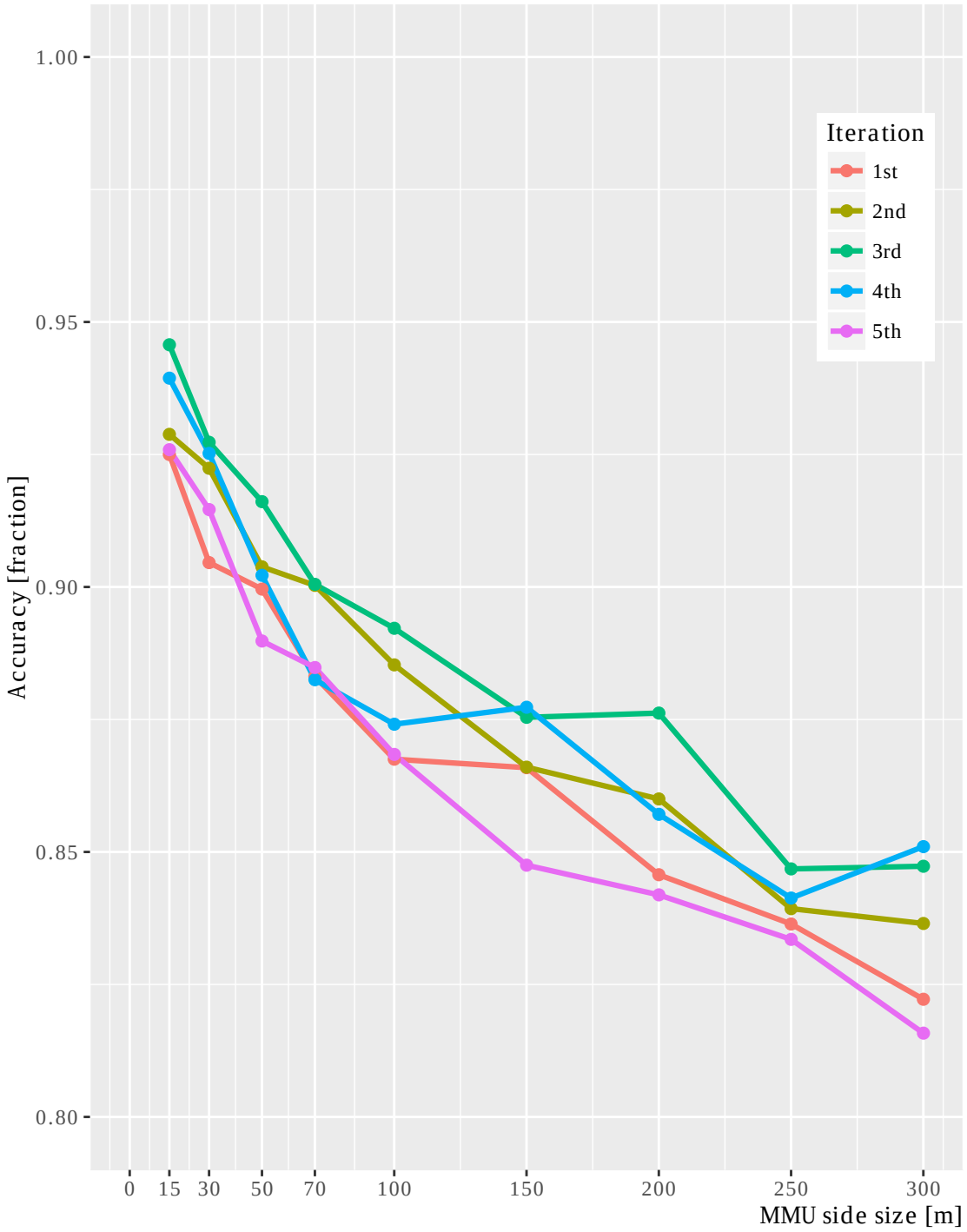

Figure 14: 5 iterations overall accuracies for all MMUs in Ethiopia